Electronic Supplementary Material (ESI) for Journal of Materials Chemistry C.

Efficient Solution-Processed Deep-blue with $CIE_y \in$ (0.05) and Pure-white $CIE_{x,y} \in$ (0.34, 0.32) Organic Light-emitting Diodes: Experimental and Theoretical Investigation

Jairam Tagare[a], Rohit Ashok Kumar Yadav[b], Sujith Sudheendran Swayamprabha[b], Deepak Kumar Dubey[b], Jwo-Huei Jou[b] and Sivakumar Vaidyanathan[a,*]

[a] Optoelectronics Laboratory, Department of Chemistry, National Institute of Technology Rourkela, India

[b]Department of Materials Science and Engineering, National Tsing Hua University, Hsinchu 30013, Taiwan ROC

[*] To whom correspondence should be addressed

Contents:

SI1.Experimental section

SI1.1. General Information and Measurements

SI1.2. Device fabrication and measurement

SI2. Synthesis and Characterization:

SI2.1. Synthesis of 4-(4-bromobutoxy) benzaldehyde (Intermediate-1)

Fig. S1. The ^{1}H NMR spectra of the Intermediate-1.

Fig. S2. The ^{13}C NMR spectra of the Intermediate-1.

SI2.2. Synthesis of 4-(4-(9H-carbazol-9-yl)butoxy) benzaldehyde (Intermediate-2)

Fig. S3. The ^{1}H NMR spectra of the Intermediate-2.

Fig. S4. The ^{13}C NMR spectra of the Intermediate-2.

SI2.3. General procedure for the synthesis of imidazole derivatives

SI3. NMR spectra (^{1}H,^{13}C and ^{19}F) spectra of imidazole derivatives.

Fig. S5. The ^{1}H NMR spectra of the PICFOCz.

Fig. S6. The ^{13}C NMR spectra of the PICFOCz.

Fig. S7. The ^{19}F NMR spectra of the PICFOCz.

Fig. S8. The ^{1}H NMR spectra of the BICFOCz.

Fig. S9. The ^{13}C NMR spectra of the BICFOCz.

Fig. S10. The ^{19}F NMR spectra of the BICFOCz

SI4. Mass spectra of imidazole derivatives.

Fig. S11. Mass spectra of the PICFOCz.

Fig. S12. Mass spectra of the BICFOCz.

SI5. Fourier transform infrared (FTIR) spectroscopy

Fig. S13.FTIR spectra of the imidazole derivatives.

SI6. Thermal properties

Fig. S14. Thermogravimetric curves of imidazole derivatives.

SI7. Photophysical properties of imidazole derivatives.

Fig. S15. Optical bandgap of the imidazole derivativescalculated from the solid-state diffuse reflectance spectra.

SI8. Quantum yield studies of imidazole derivatives in solution and solid-state

Fig. S16. The PLQY of the PICFOCz in solution and solid.

Fig. S17. The PLQY of the BICFOCz in solution and solid.

SI9. The calculated UV/Vis absorption spectra and vertical excitation wavelengths, orbital contribution, and oscillator strength (f) of imidazole derivatives.

Fig. S18. Calculated UV/Vis absorption spectra of the imidazole derivativesin gas (a) and DCM solution (b) phase.

SI10. DFT calculation of BPA-BPI, TPA-BPI, TPA-PIM, and M1 molecules:

Fig. S19. Optimized structures of BPA-BPI, TPA-BPI, TPA-PIM, and M1 molecules.

Fig. S20. Frontier molecular orbitals (FMO) comparition spectra.

SI10. Electroluminescence characteristics

Fig. S21. (a) Luminance-voltage, (b) current density-voltage, (c) current efficiency-luminance, (d) power efficiency-luminance, and (e) normalized EL spectra plots of the solution-processed deep-blue OLED devices based on different doping concentration of PICFOCz within CBP host.

Fig. S22. (a) Luminance-voltage, (b) current density-voltage, (c) current efficiency-luminance, (d) power efficiency-luminance, and (e) normalized EL spectra plots of the solution-processed deep-blue OLED devices based on different doping concentration of BICFOCz within CBP host.

Fig. S23. Schematic illustration of the energy levels of the solution-processed deep-blue OLED devices composing 0.5 wt% BICFOCz emitters in different host molecules, CBP, mCP, TCTA, and Spiro-2CBP.

Fig. S24. (a) Luminance-voltage, (b) current density-voltage, (c) current efficiency-luminance, (d) power efficiency-luminance, and (e) normalized EL spectra plots of the 0.5 wt% BICFOCz based solution-processed deep-blue OLED devices in different host matrix.

Fig. S25.(a) Current density-voltage, (b) luminance-voltage, (c) current efficiency-luminance, and (d) power efficiency-luminance plots of the solution-processed white-OLED devices using BICFOCz and Ir(2-phq)$_3$ as a near-UV and orange-red, respectively.

Fig. S26. Phosphorescence spectra of films recorded on fluorescence spectrophotometer at 77 K.

Fig. S27. AFM images of the surfaces morphology of the films that comprise 0.5 wt% (a) PICFOCz and (b) BICFOCz doped in CBP host matrix.

SI11. Atom coordinates of imidazole derivatives.

SI1.Experimental section

SI1.1. General Information and Measurements:

Commercially available reagents (Sigma Aldrich) were used without further purification unless otherwise stated. All the reactions were monitored by thin-layer chromatography (TLC) with silica gel 60 F_{254} Aluminium plates (Merck). Column chromatography was carried out using silica gel. ^{1}H-NMR, ^{13}C-NMR, and^{19}F-NMR spectra were recorded using an AV 400 Avance-III 400MHz FT-NMR Spectrometer (Bruker Biospin International, Switzerland) with tetramethylsilane (TMS) as a standard reference. The FTIR spectra were recorded on a Shimadzu IR Affinity-1S spectrophotometer. Elemental analysis was obtained using Elementary Analysis System, Germany/Vario EL spectrometer. The mass spectra were recorded by LC–MS (Perkin–Elmer, USA/Flexer SQ 300 M). The absorption spectrum of the target fluorophores in the solution phase and solid (DRS) were measured by using UV-visible spectrometer (Shimadzu Corporation, Japan/UV-2450 Perkin Elmer, USA/Lamda 25). The photoluminescence excitation and emission spectra were recorded by Horiba Jobin Yvon, USA/Fluoromax 4P spectrophotometer. The absolute quantum yields were determined by using Edinburgh Instruments, spectrofluorometer, FS5, Integrating Sphere SC-30. The CIE color coordinates were calculated by using PL emission data (MATLAB software). The electrochemical properties of the fluorophores were measured by using cyclic voltammetry (CV), AUTOLAB 302N Modular potentiostat, at RT in dimethylformamide (DMF). The working (glass-carbon rod), auxiliary (counter, Pt wire), and reference (Ag/AgCl wire) electrodes were used for CV analysis. The

DMF which contains 0.1 M Bu_4NClO_4 was used as the supporting electrolyte, and the scan rate was maintained as 100 mV s^{-1}. The optimized structures and HOMO-LUMO energy levels of the fluorophores were calculated by using DFT calculation with B3LYP/6-31G (d, p) basis set. After confirming the ground state geometry of the fluorophores, we were vertically excited the fluorophores to get the first excited state using time-dependent density functional theory (TD-DFT).

SI1.2. Device fabrication and measurement:

The device fabrication involved both spin coating and thermal evaporation (under less than 10^{-5} Torr). First, spin coating of an aqueous solution of poly(3,4-ethylenedioxythiophene) polystyrene sulfonate (PEDOT: PSS) at 4,000 rpm for 20 s to form a thin film of hole injection layer on pre-treated Indium tin oxide (ITO) anode. The emissive layer (EML) solution was prepared by dissolving the 4,4′-Bis(N-carbazolyl)-1,1′-biphenyl (CBP) host and guest dopants in tetrahydrofuran (THF) at 50 ^{0}C for 30 min under stirring. The EML solution was spin-coated at 2,500 rpm for 20 s under a nitrogen atmosphere. The electron transporting layer TPBi, the electron injection layer LiF, and the cathode Al by thermal evaporation.

The device characteristics; luminance, color coordinates (CIE coordinates), and electroluminescence (EL) spectrum were measured by Photo Research PR-655 spectra scan. The current-voltage (I-V) characteristics were measured by Keithley 2,400. The device area was 0.9 mm^2 and all the devices measured in the forward bias.

SI2. Synthesis and Characterization

SI2.1. Synthesis of 4-(4-bromobutoxy) benzaldehyde (Intermediate-1): In the two necks round bottom flask 4-hydroxybenzaldehyde (2.5 g, 1 eq) and acetonitrile 30 mL were taken. To this reaction mixture potassium carbonate (5.69 g, 2 eq) was added. Then after 10 minutes, 1,4-

dibromo butane (4.42 g, 1 eq) was added to the reaction mixture. The resulting reaction mixture was stirred for 48 hr at 85 ^{0}C under a nitrogen atmosphere. The reaction was monitored by thin-layer chromatography (ethyl-acetate (EtOAc) in pet ether 1:9) for the completion of the reaction. After completion of the reaction, the reaction mixture was poured in a minimum amount of water and extracted with an ethyl-acetate solvent. The solvent was evaporated to get the yellow color crude compound. The obtained crude compound was purified by column chromatography by using silica gel (100-200 mesh), eluent ethyl-acetate in pet ether (1:9). Yield 80 %, the semisolid compound obtained. ^{1}H-NMR (400 MHz, $CDCl_3$, TMS, δ ppm): 9.85 (s, 1H), 7.82-7.79 (m, 2H), 6.95 (t, 2H), 4.06 (t, 2H), 3.47 (t, 2H), 2.04-2.00 (m, 2H), 1.99-1.88 (m, 2H), ^{13}C-NMR (100 MHz, $CDCl_3$, TMS, δ ppm): 190.82, 163.90, 132.01, 129.92, 114.74, 114.72, 68.02, 33.29, 29.29, 27.69.

SI2.2. Synthesis of 4-(4-(9H-carbazol-9-yl)butoxy) benzaldehyde (Intermediate-2): The mixture of 4-(4-bromobutoxy) benzaldehyde (3 g, 1 eq), 9H-carbazole (1.94 g, 1 eq),and tetrahydrofuran (THF) (25 mL) was taken in 100 ml two necks round bottom flask. Then potassium hydroxide (1.96 g, 3 eq) base was added. Followed by added tetrabutylammonium bromide (0.15 g, 0.04 eq) water (5 mL) solution to the reaction mixture. The resulting reaction mixture was refluxed 18 hr. The completion of the reaction was monitored by thin-layer chromatography (ethyl-acetate (EtOAc) in pet-ether 1:9). After completion of the reaction, the reaction mixture was poured in a minimum amount of water and extracted with an ethyl-acetate solvent. The solvent was evaporated to get the yellow color crude compound. The obtained crude compound was purified by column chromatography by using silica gel (100-200 mesh), eluent ethyl-acetate in pet-ether (1:9). Yield 50 %, the pale yellow color compound obtained. ^{1}H-NMR (400 MHz, $CDCl_3$, TMS, δ ppm): 9.86 (s, 1H), 8.12 (d, 2H), 7.79 (t, 2H), 7.50-7.41 (m, 4H),

7.25 (t, 2H), 6.92 (d, 2H), 4.41 (t, 2H), 3.98 (t, 2H), 2.13-2.06 (m, 2H), 1.90-1.83 (m, 2H), ^{13}C-NMR (100 MHz, $CDCl_3$, TMS, δ ppm): 190.89, 163.89, 140.34, 132.03, 129.89, 125.72, 122.90, 120.48, 114.67, 108.61, 67.84, 42. 64, 26.86, 25.79.

SI2.3. General Procedure for the synthesis of imidazole derivatives:

A mixture of intermediate-2 (0.50 g, 1 eq), 9,10-phenanthrenequinine (0.30 g, 1 eq)/benzil (0.36 g, 1 eq),3-(trifluoromethyl)benzenamine (0.17 g, 1.3 eq) and ammonium acetate (1.16 g, 10 eq) and acetic acid (30 mL) were refluxed for 12 hr, under nitrogen in an oil bath. After completion of the reaction, the mixture was cooled and poured a minimum amount of water. The corresponding reaction mixture was neutralized with dilute ammonium hydroxide solution. The resultant mixture was extracted with dichloromethane (DCM) followed by purification by column chromatography on silica gel (100-200 mesh) with ethyl acetate/petroleum ether (2:8) as the eluent.

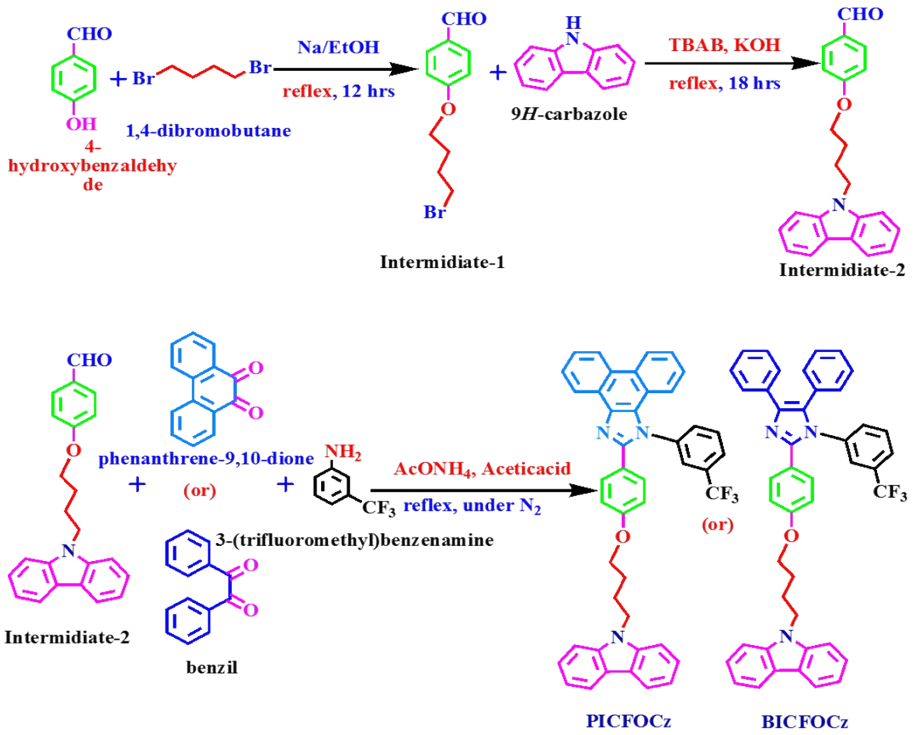

Scheme S1. Synthetic routes of imidazole derivatives.

Synthesis of 2-(4-(4-(9H-carbazol-9-yl)butoxy)phenyl)-1-(3-(trifluoromethyl)phenyl)-1H-phenanthro [9,10-d]imidazole (PICFOCz): Yield: 75%,white color, ^{1}H-NMR (400 MHz, $CDCl_3$, TMS, δ ppm): 8.87 (d, *J*=7.6 Hz, 1H), 8.80 (d, *J*=8.4 Hz, 1H), 8.73 (d, *J*=8.0 Hz, 1H), 8.13 (d, *J*=8.0 Hz, 2H), 7.90 (d, *J*=7.6 Hz, 1H), 7.81-7.66 (m, 6H), 7.56-7.24 (m, 9H), 7.10 (d, *J*=8.4 Hz, 1H), 6.79 (d, *J*=8.8 Hz, 2H), 4.41 (t, J=6.8 Hz, 2H), 3.94 (t, J=6.0 Hz, 2H), 2.13-2.08 (m, 2H), 1.89-1.83 (m, 2H), ^{13}C-NMR (100 MHz, $CDCl_3$, TMS, δ ppm): 159.39, 140.37, 132.66, 130.90, 130.74, 129.26, 128.30, 127.63, 127.36, 126.38, 125.76, 125.68, 124.95, 124.31, 123.11, 122.81, 120.41, 120.36, 118.88, 114.36, 108.60, 67.52, 42.20, 32.20, 26.92, 25.82 and ^{19}F-NMR (400 MHz, $CDCl_3$, TMS, δ ppm) -62.69 (s, 3F). FTIR (KBr, υ/cm^{-1}): 3427, 3067, 2944, 1611, 1466, 1335, 1251, 1182, 1130, 1067, 830, 722, 561. CHNS Elemental Analysis: Anal. Calc. for $C_{44}H_{32}F_3N_3O$: C, 78.21; H, 4.77; N, 6.22; Found: C, 78.47; H, 5.99; N, 6.36 %.EI-MS: m/z exp. (calc.). 675.74 found 695.07 $[M+H_2O]^+$.

9-(4-(4-(1-(3-(trifluoromethyl)phenyl)-4,5-diphenyl-1H-imidazol-2-yl)phenoxy)butyl)-9H-carbazole (BICFOCz): Yield: 65%,pale brown color solid, ^{1}H-NMR (400 MHz, $CDCl_3$, TMS, δ ppm): 8.13 (d, *J*=7.6 Hz, 2H), 7.73 (d, *J*=7.6 Hz, 2H), 7.59-7.54 (m, 2H), 7.50-7.34 (m, 8H), 7.28-7.19 (m, 8H), 7.11 (d, *J*=6.8 Hz, 2H), 6.74 (d, *J*=8.4 Hz, 2H), 4.41 (t, *J*=6.8 Hz, 2H), 3.91 (t, *J*=6.0 Hz, 2H), 2.10-2.06 (m, 2H), 1.87-1.82 (m, 2H), ^{13}C-NMR (100 MHz, $CDCl_3$, TMS, δ ppm):159.26, 147.08, 140.34, 138.55, 138.38, 137.58, 133.98, 131.66, 131.66, 131.35, 131.06, 130.48,130.23, 130.03, 129.71, 129.47, 128.62, 128.34, 128.28, 127.48, 126.92, 125.70, 125.33, 124.85, 122.90, 122.85, 122.27, 120.72, 120.42, 118.87, 116.50, 114.28, 108.64, 67.46, 42.68, 32.45, 26.90, 25.83 and^{19}F-NMR (400 MHz, $CDCl_3$, TMS, δ ppm) -62.68 (s, 3F). FTIR (KBr, ν / cm^{-1}): 3415, 3051, 2937, 2875, 1604, 1489, 1450, 1335, 1251, 1174, 1130, 1067, 799, 745, 695,

538.CHNS Elemental Analysis: Anal. Calc. for $C_{44}H_{34}F_3N_3O$: C, 77.97; H, 5.06; N, 6.20; Found: C, 78.13; H, 5.31; N, 6.43 %. EI-MS: m/z exp. (calc.). 677.76 found 678.86 $[M]^+$

SI3. NMR spectra (^{1}H,^{13}C and ^{19}F) spectra of PI derivatives

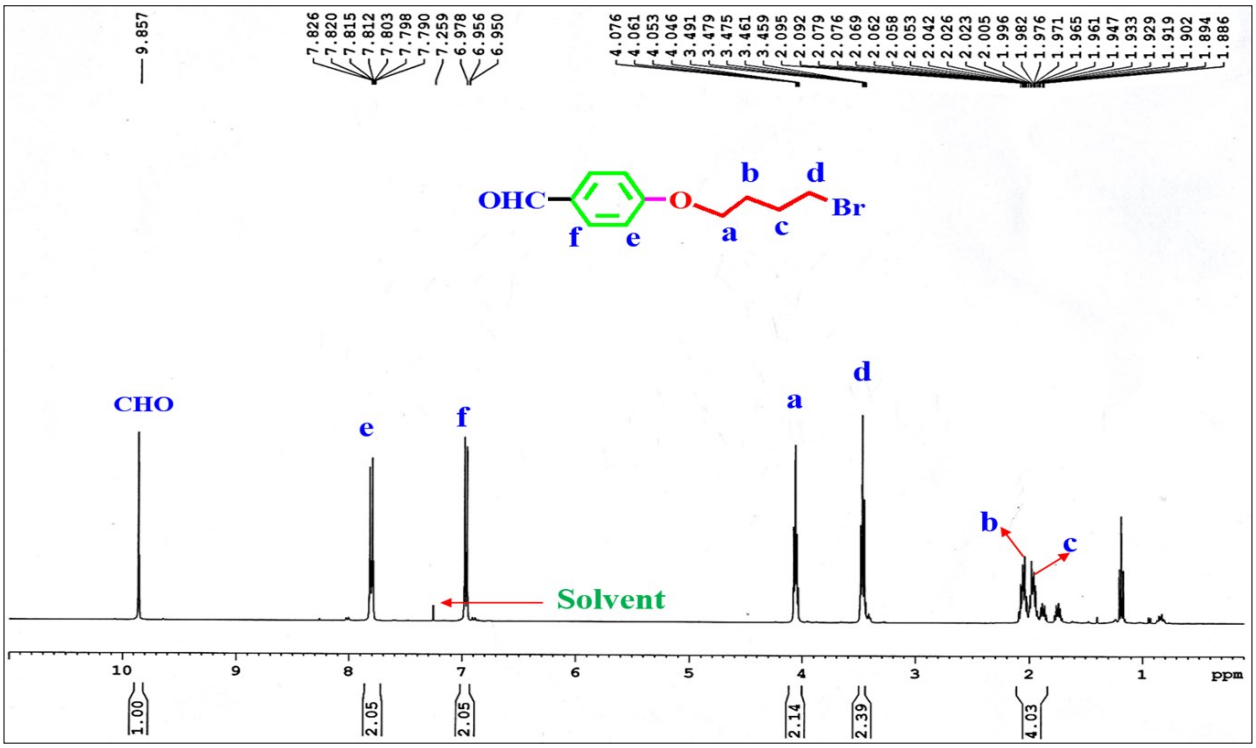

Fig. S1. The ^{1}H NMR spectra of the Intermediate-1.

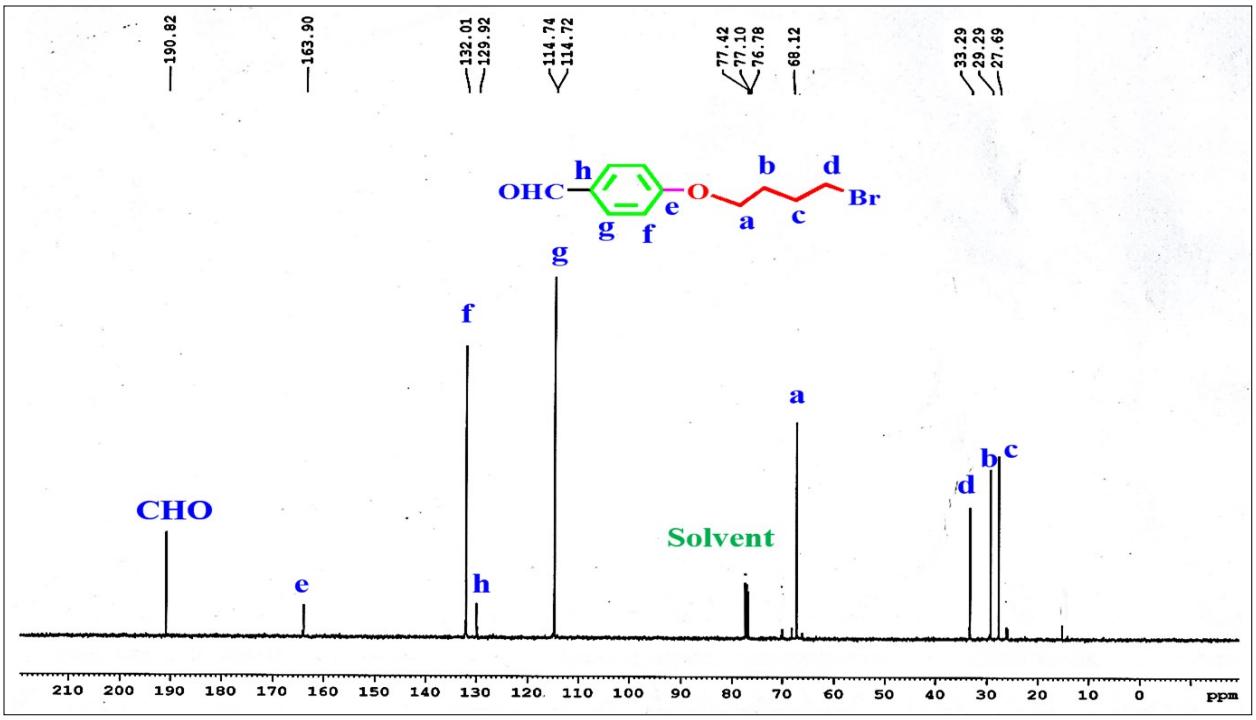

Fig. S2. The ^{13}C NMR spectra of the Intermediate-1.

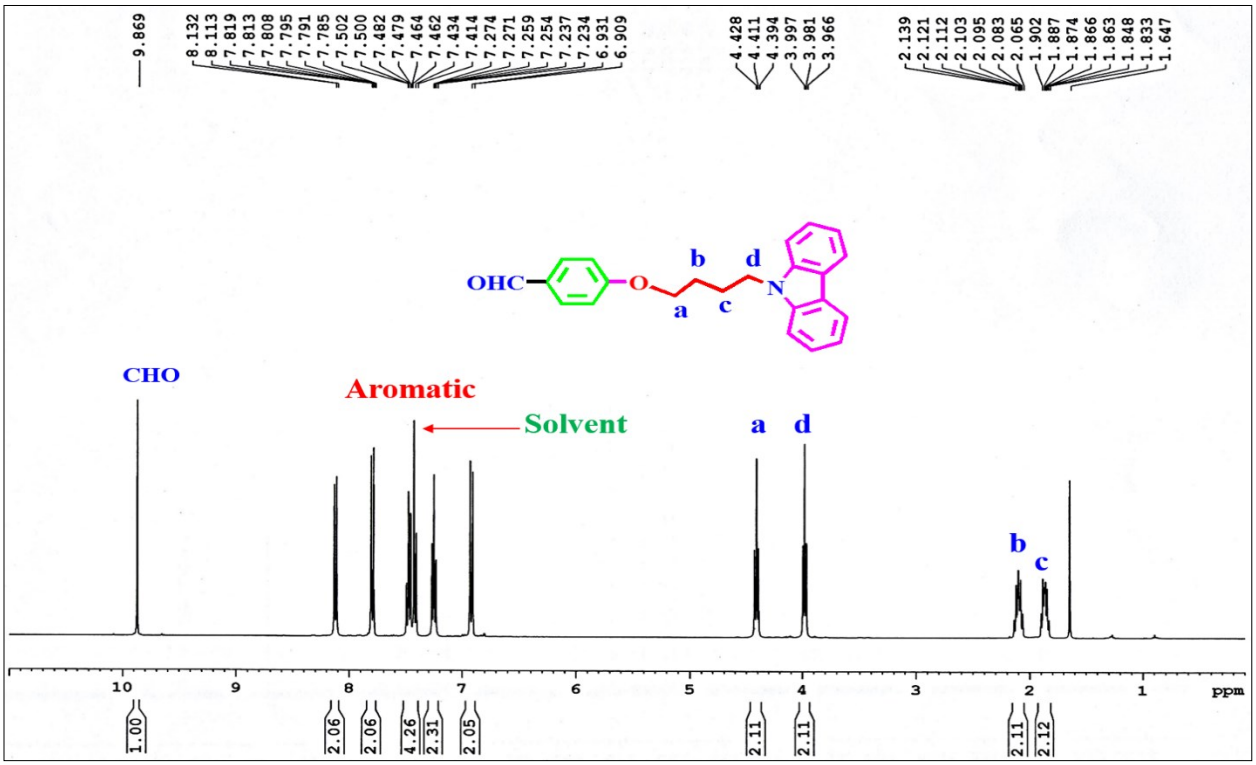

Fig. S3. The ^{1}H NMR spectra of the Intermediate-2.

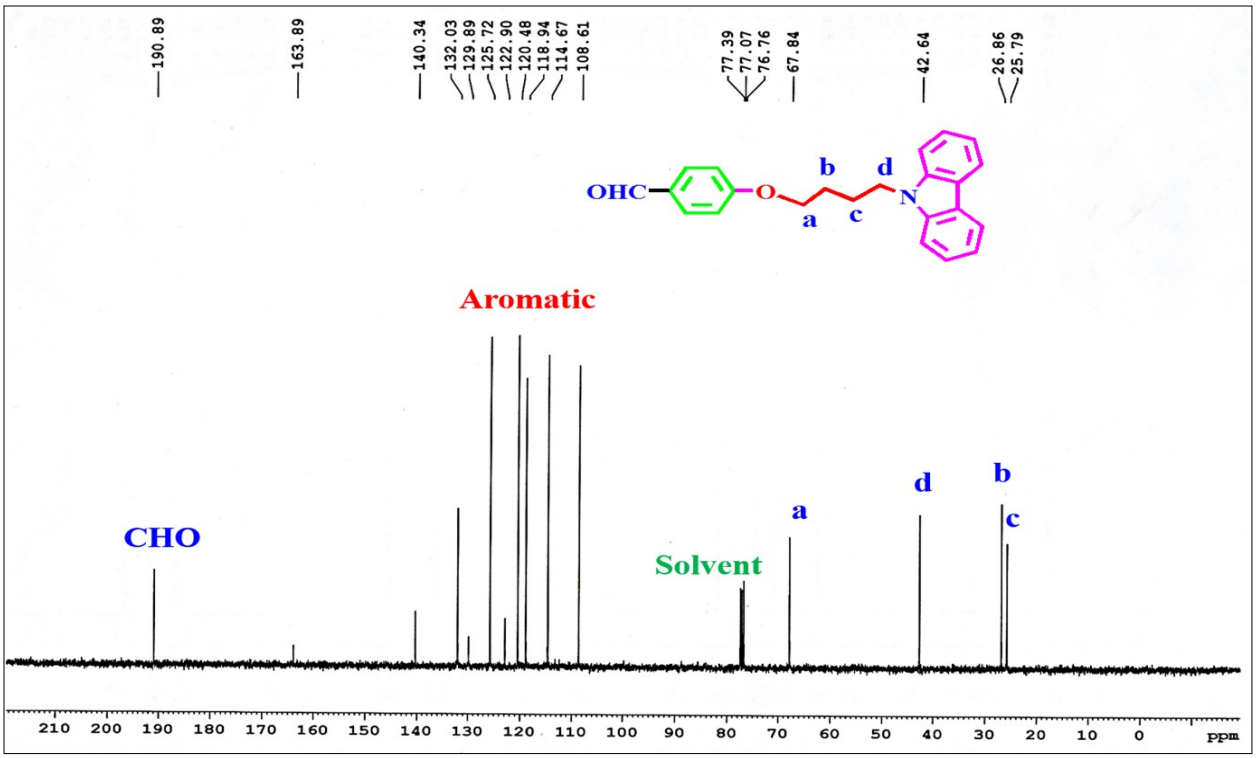

Fig. S4. The ^{13}C NMR spectra of the Intermediate-2.

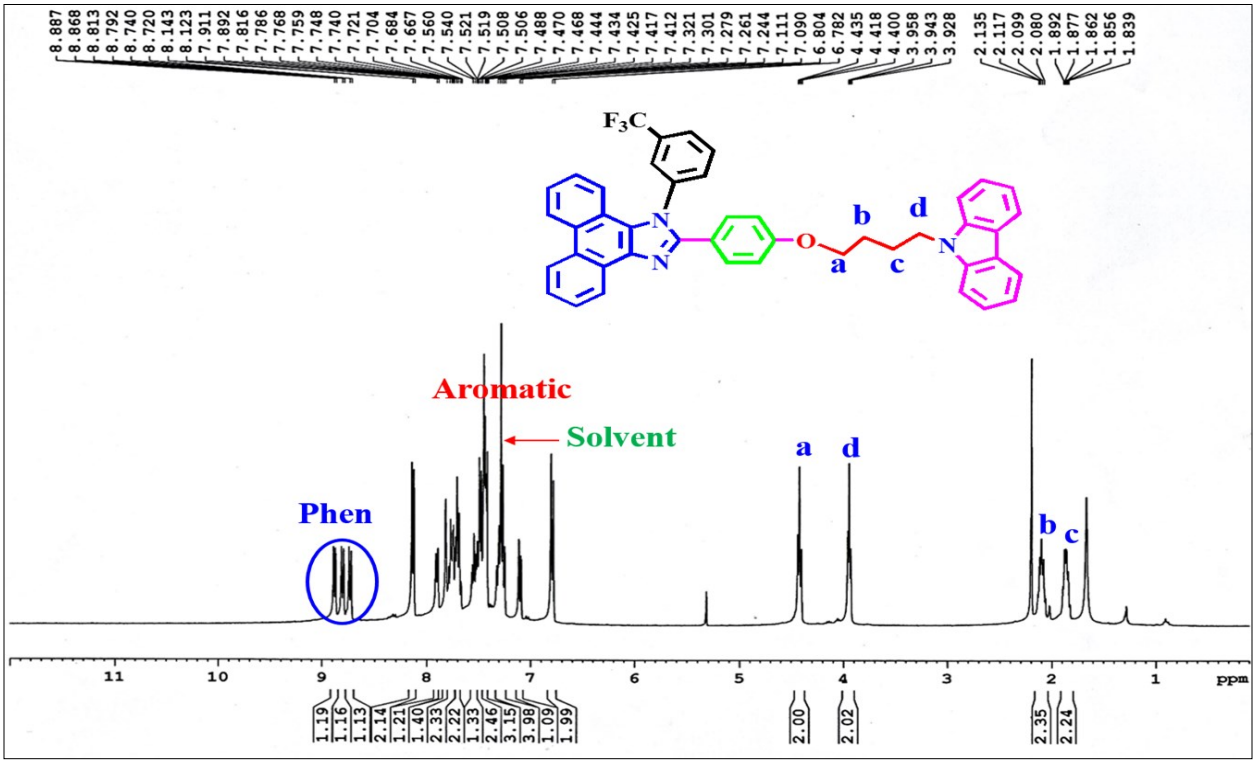

Fig. S5. The ^{1}H NMR spectra of the PICFOCz

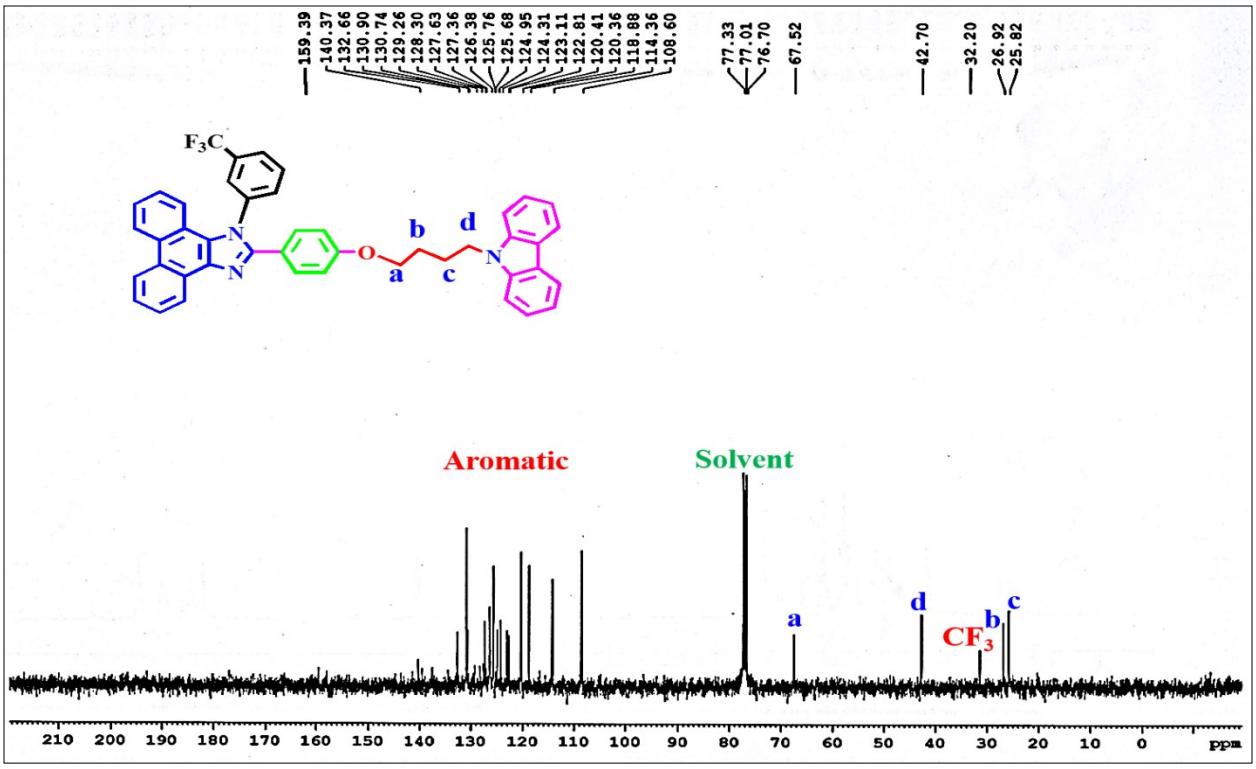

Fig. S6. The [13]CNMR spectra of the PICFOCz

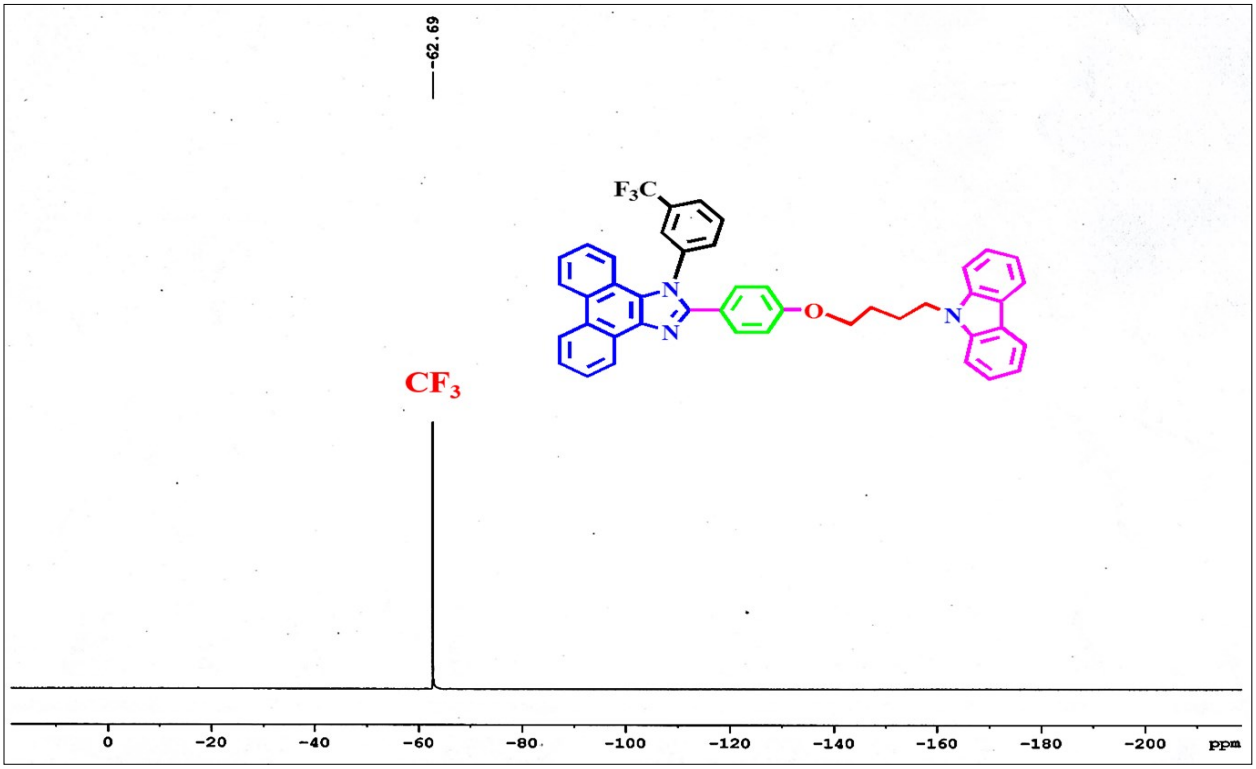

Fig. S7. The [19]FNMR spectra of the PICFOCz

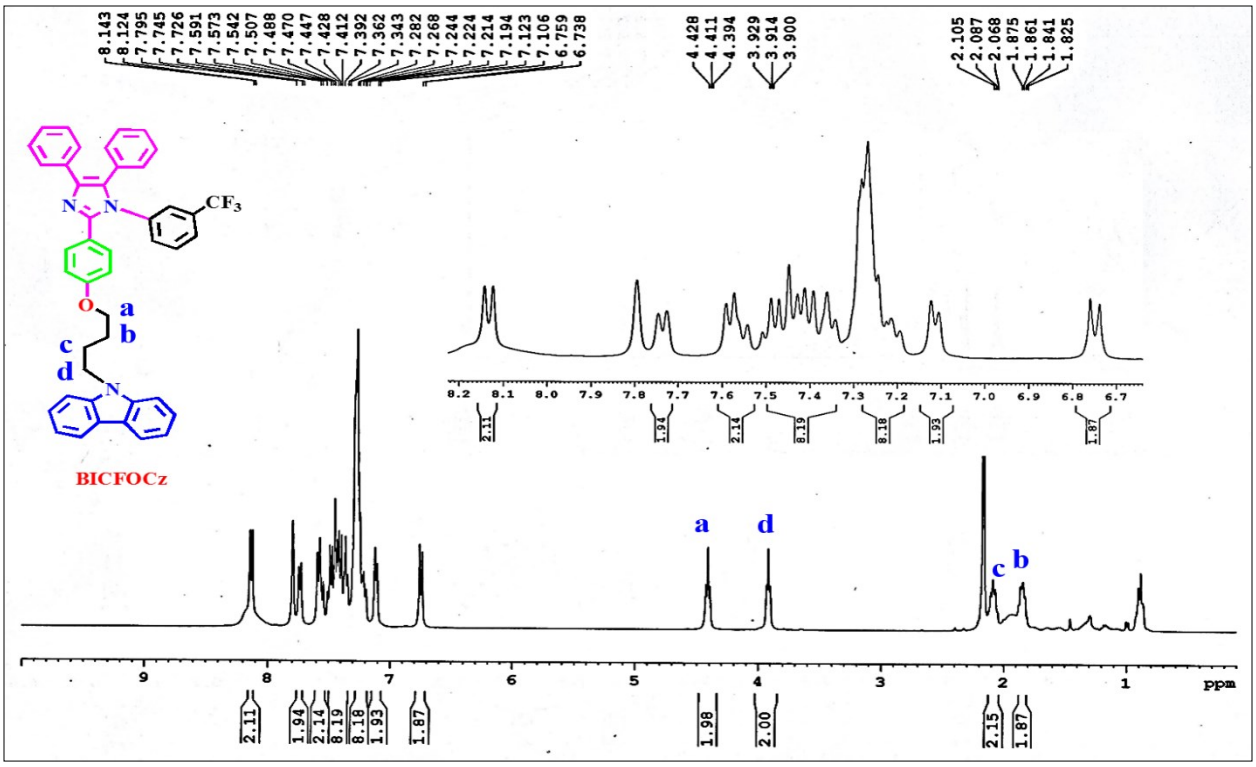

Fig. S8. The ^{1}H NMR spectra of the BICFOCz compound.

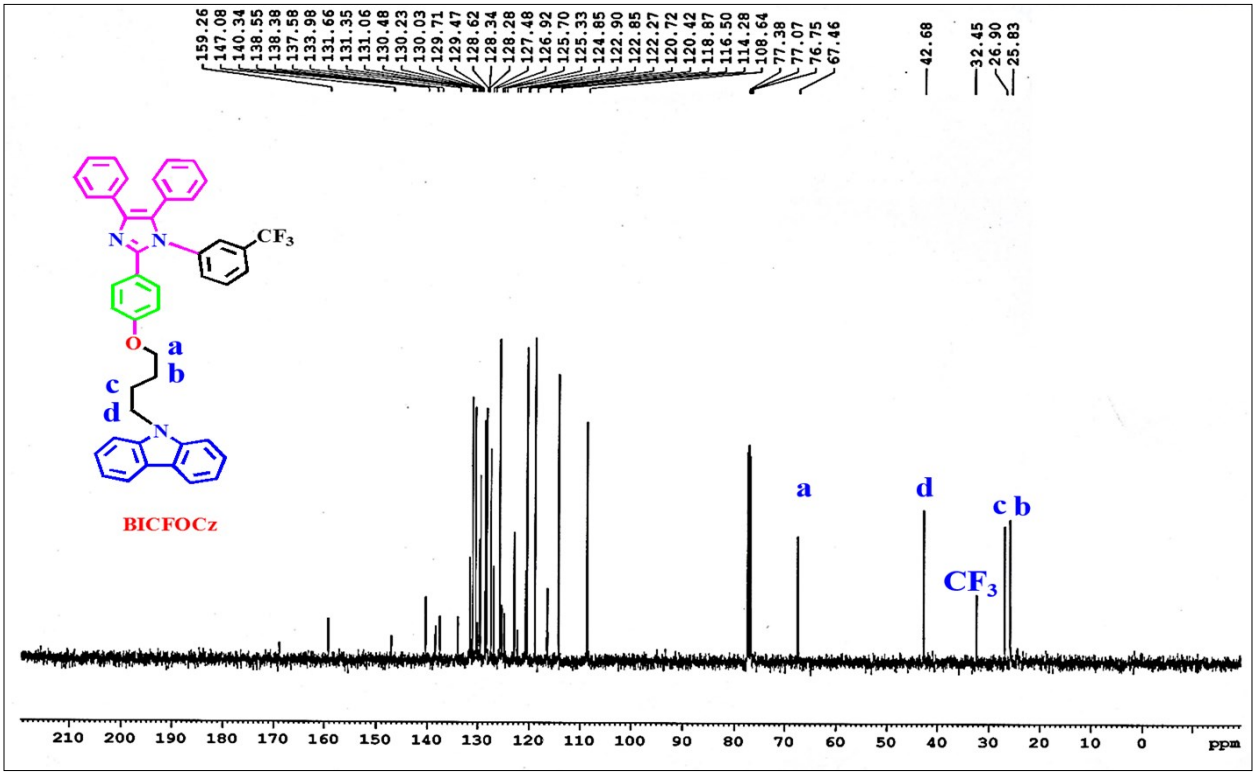

Fig. S9. The ^{13}C NMR spectra of the BICFOCz compound.

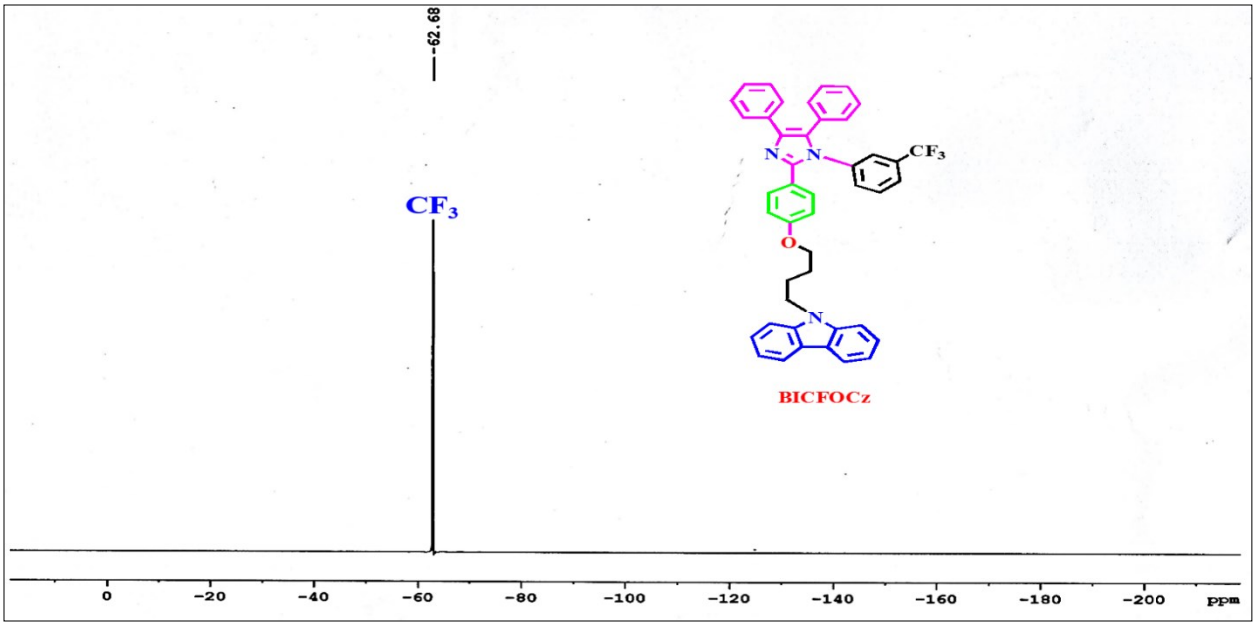

Fig. S10. The ^{19}F NMR spectra of the BICFOCzcompound.

SI4. Mass spectra of PI derivatives.

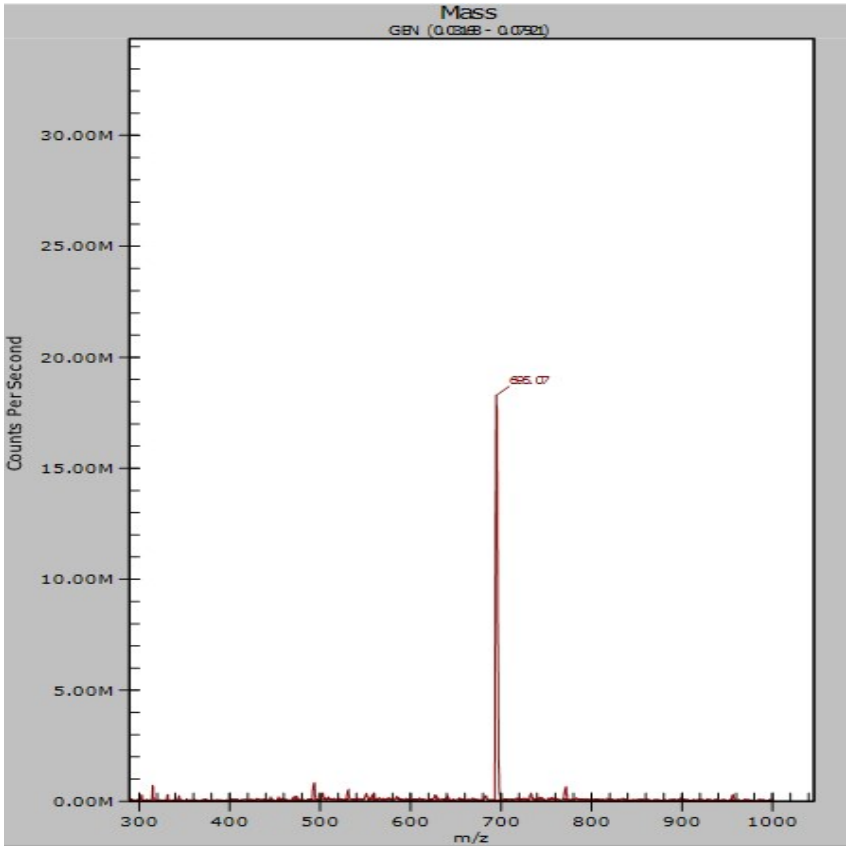

Fig. S11. Mass spectra of the PICFOCz.

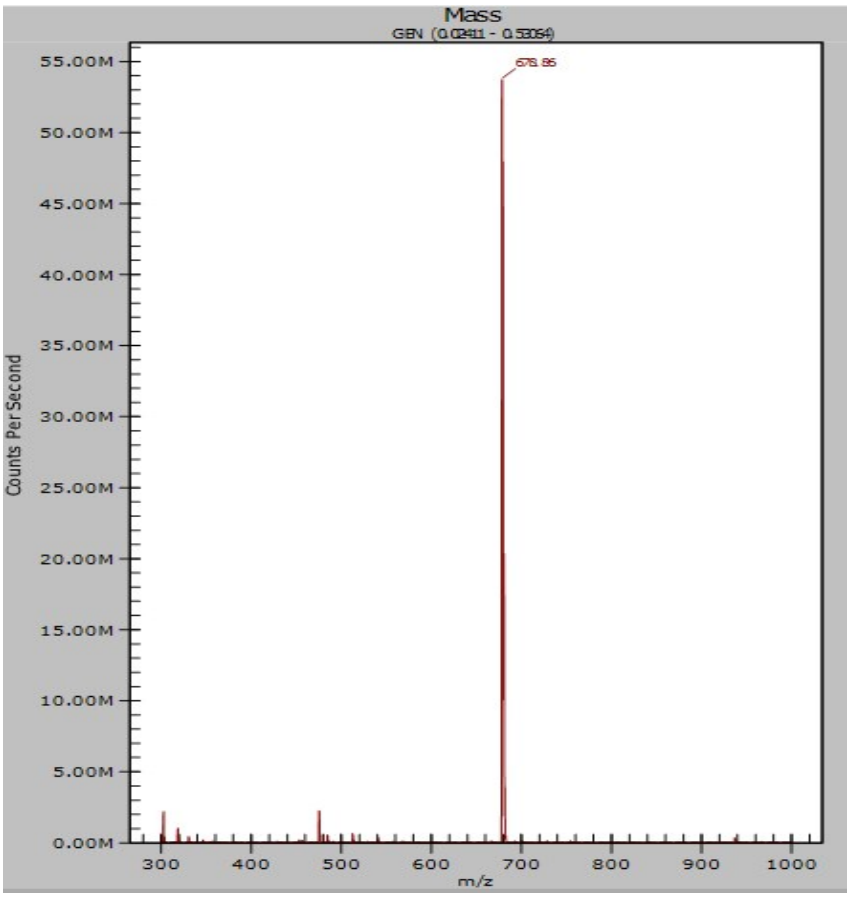

Fig. S12. Mass spectra of the BICFOCz compound.

SI5. Fourier transform infrared (FTIR) spectroscopy:

The FTIR spectra of synthesized luminogens were recorded at the spectral window of the 400-4000 $cm^{-1}$and corresponding spectra are sown in Fig. S13 and major bands wavenumbers are displayed in Table S1. The frequency at 1604 cm^{-1} corresponds to the C=N functional group of the imidazole moiety. The peak around 3400 cm^{-1} corresponds to ≥ C–H functional group in all the compounds [1]. The frequency around 1250cm^{-1}corresponding to the alkyl C-H functional group and the stretching frequency around 2900 cm^{-1}corresponds to the alkyl C-H functional group. The frequency at 1132 cm^{-1} corresponds to the CF_3 group in BICFOCz compound. The frequency in the range of 500 to 900 cm^{-1}corresponds to the aromatic C-H bending frequency.

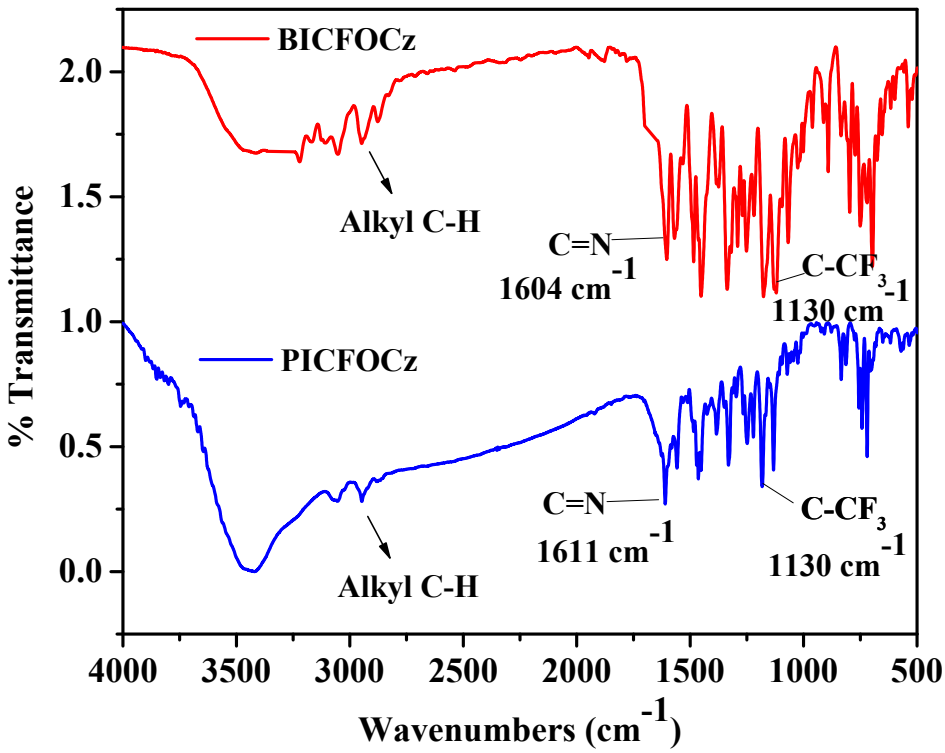

Fig. S13.FTIR spectra of the imidazole derivatives.

Table S1. The major FTIR bands [cm^{-1}] for the imidazolederivatives

Bonding	PICFOCz	BICFOCz
C=N stretch	1611	1604
C-CF_3	1130	1130
C-N stretch	1251	1251
C-O stretch	1067	1067
NH–CH	3427	3415
Aromatic C-H, C-C, C=C, stretching frequency	3067, 1466, 1335, 1182	3051, 1489, 1450, 1335, 1174
Alkyl C-H stretch	2944	2937, 2875
C–H bending frequency	830, 722, 561	799, 745, 695, 538

SI6.Thermal properties

Thermal properties of PICFOCz and BICFOCz fluorophores were investigated by using thermogravimetric analysis (TGA). As shown in Fig. S14, the thermal decomposition temperature (Td, with 5% weight loss) of PICFOCz and BICFOCz are 305°C and 246 °C, respectively. The obtained Td values ensure that good thermal stability during the heating and annealing of the solution process. Among both the fluorophores, PICFOCz fluorophore show high thermal stability, due to consist of thermally stable rigid phenanthrene moiety in the molecular structure and BICFOCz fluorophore having a more flexible nature, due to more phenyl groups integrated on imidazole moiety, which is the main reason for the more Td of PICFOCz (Table 1).

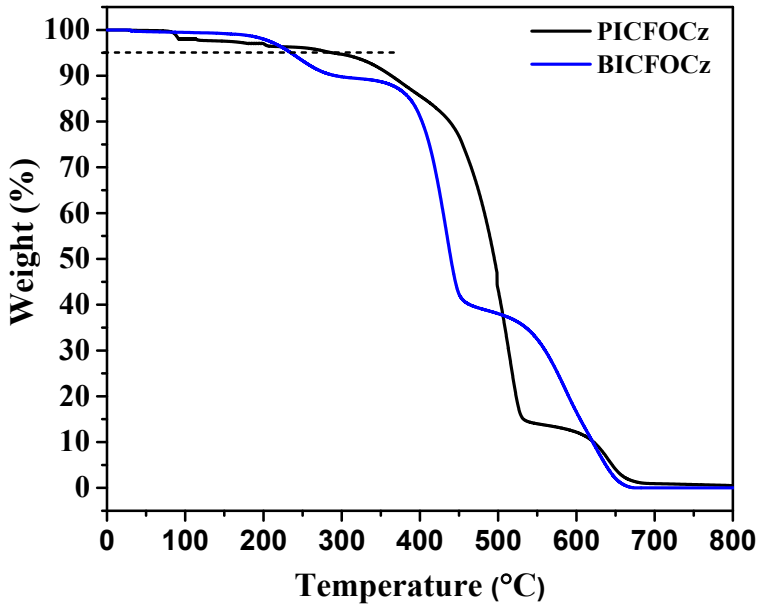

Fig. S14. Thermogravimetric curves of imidazole derivatives.

SI7. Photophysical properties of PI derivatives

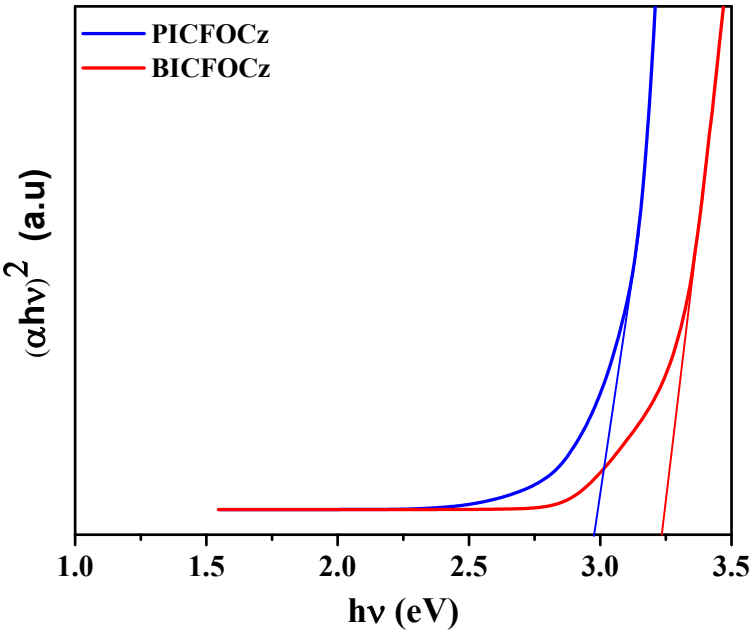

Fig. S15. Optical bandgap of the fluorophores calculated from the solid-state diffuse reflectance spectra

SI8. Quantum yield studies of PI derivatives in solution and solid-state

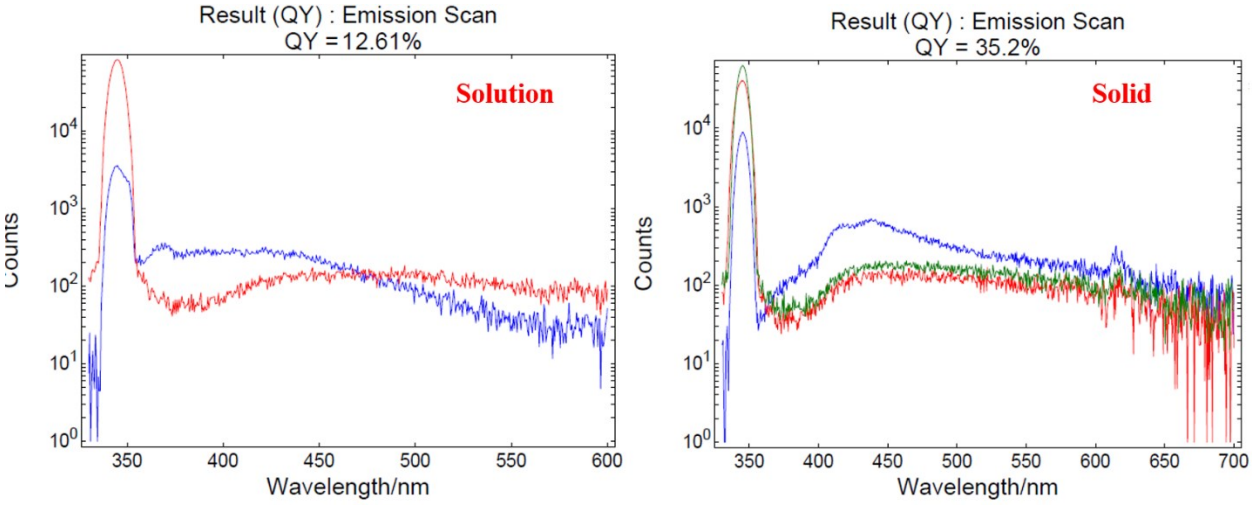

Fig. S16. The PLQY of the PICFOCz in solution and solid.

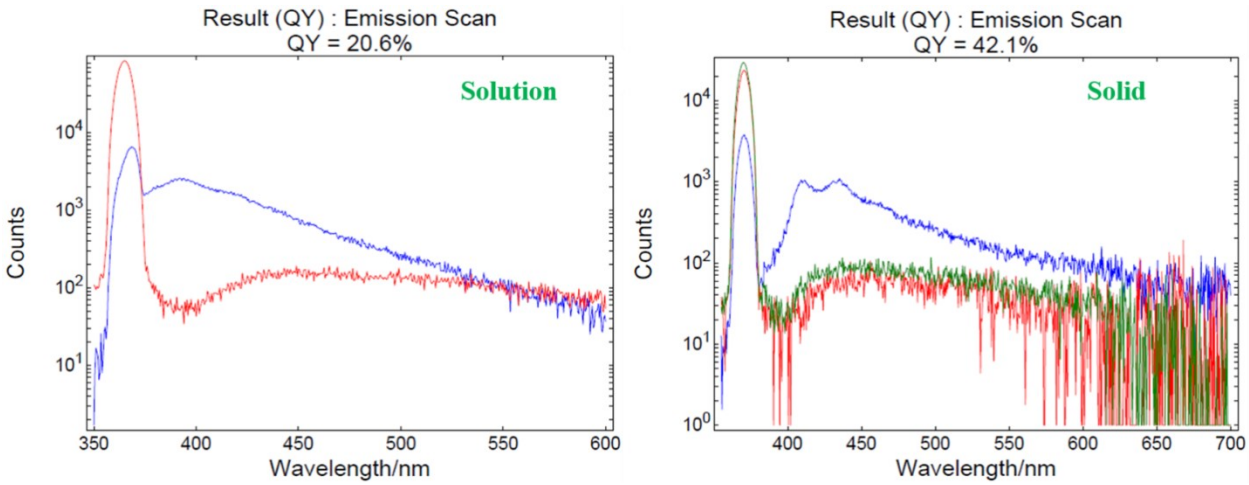

Fig. S17. The PLQY of the BICFOCz compound in solution and solid.

SI9. The calculated UV/Vis absorption spectra and vertical excitation wavelengths, orbital contribution and oscillator strength (f) of PI derivatives.

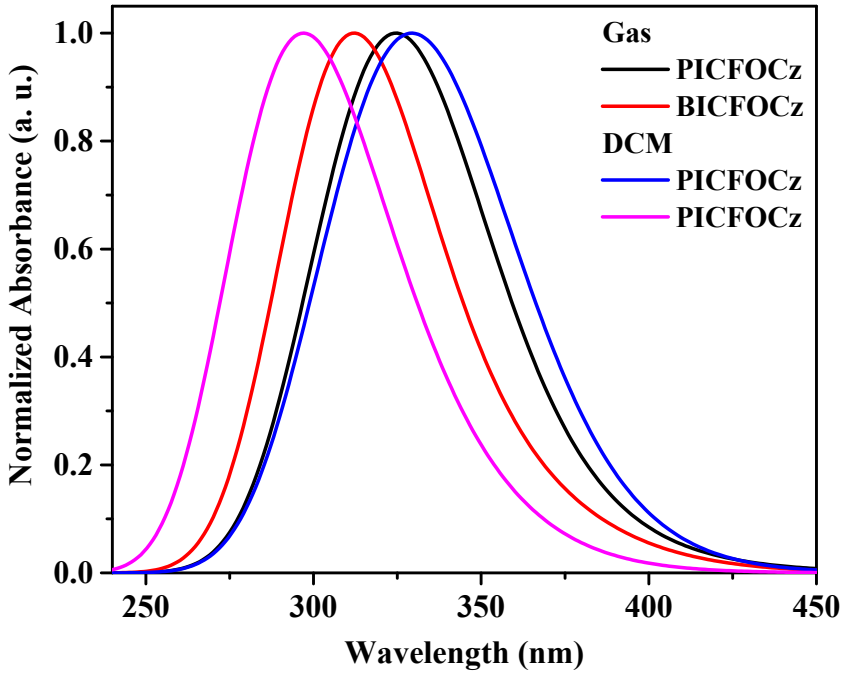

Fig. S18. Calculated UV/Vis absorption spectra of the fluorophores in gas (a) and DCM solution (b) phase.

Table S2.The computed vertical transitions and there oscillator strengths (*f*) and configuration of the PICFOCz fluorophore.

Fluorophore	State	Energy (eV)	λ_{max} nm	*f*	Configuration
PICFOCz Singlet	Gas	3.2548	380.92	0.0160	HOMO→ LUMO(70.20%)
		3.7078	334.38	0.2554	HOMO-3→ LUMO+1 (10.76%) HOMO-3→ LUMO+5(11.30%) HOMO→ LUMO+1(13.94%) HOMO→ LUMO+2 (54.03%) HOMO→ LUMO+3 (35.56%)
		3.8958	318.25	0.3401	HOMO-3→ LUMO+1 (13.25%) HOMO-3→ LUMO+2 (17.83%) HOMO→ LUMO+3 (52.74%)
Triplet	Gas	2.7023	458.80	-	HOMO→ LUMO (24.04%) HOMO→ LUMO+1 (33.93%) HOMO→ LUMO+2 (38.67%)
Singlet	DCM	3.5314	351.09	0.0582	HOMO→ LUMO (66.99%) HOMO→ LUMO+1 (20.67%)
		3.6573	339.00	0.4124	HOMO→ LUMO+1 (61.45%) HOMO→ LUMO+2 (16.80%) HOMO→ LUMO+3 (15.10%)
		3.9250	315.88	0.3154	HOMO-3→ LUMO+1 (17.21%) HOMO→ LUMO+3 (63.54%)
Triplet	DCM	2.7351	453.31	-	HOMO-4→ LUMO+5 (14.64%) HOMO→ LUMO+1 (39.44%)

Table S3.The computed vertical transitions and their oscillator strengths (f) and configuration of the BICFOCz compound.

Compound	State	Energy (eV)	λ_{max} nm	f	Configuration
BICFOCz Singlet	Gas	3.4363	360.81	0.0254	HOMO→ LUMO (70.20%)
		3.6520	339.49	0.0291	HOMO→ LUMO+1 (68.97%) HOMO→ LUMO+3(14.15%)
		3.9906	310.69	0.1663	HOMO-1→ LUMO (46.95%) HOMO→ LUMO+3 (50.13%)
		3.9920	310.59	0.1320	HOMO-1→ LUMO (52.82%)
		4.0313	307.55	0.0255	HOMO-2→ LUMO+8 (17.23%) HOMO-1→ LUMO+2(67.60%)
Triplet	Gas	2.8614	433.30	-	HOMO-3→ LUMO+4 (15.70%) HOMO→ LUMO+3 (41.38%)
Singlet	DCM	3.6405	340.57	0.0756	HOMO→ LUMO (69.80%)
		3.8620	321.04	0.0815	HOMO→ LUMO+1 (66.67%) HOMO→ LUMO+3 (21.91%)
		4.0343	307.32	0.2817	HOMO→ LUMO+3 (65.53%)
		4.2957	288.62	0.5822	HOMO→ LUMO+4 (69.36%)
Triplet	DCM	2.9093	426.16	-	HOMO→ LUMO (45.24%) HOMO→ LUMO+1 (29.25%) HOMO→ LUMO+7(12.88%)

SI9. DFT calculation of BPA-BPI, TPA-PPI, TPA-PIM, M1 and mTPA-PPImolecules:

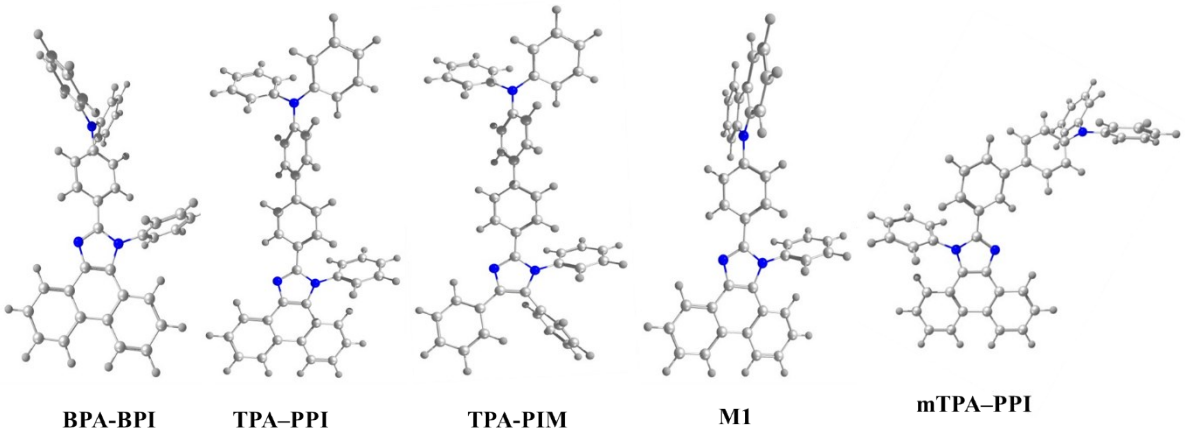

Fig. S19. Optimized structures of BPA-BPI, TPA-PPI, TPA-PIM, M1 and mTPA-PPI molecules.

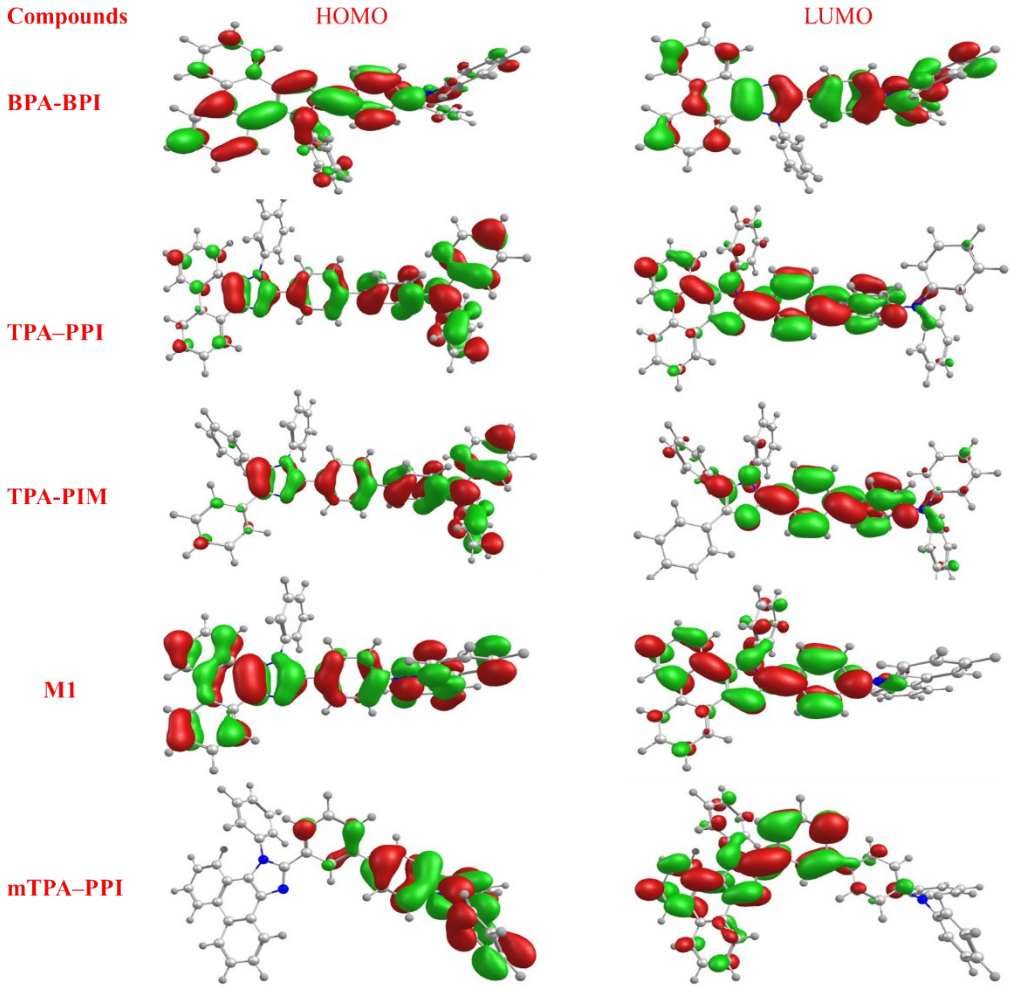

Fig. S20. Frontier molecular orbitals (FMO)comparition spectra.

SI10. Electroluminescence characteristics

Table S4. Effect of doping concentration on the turn-on voltage, power efficiency (PE), current efficiency (CE), external quantum efficiency (EQE), CIE coordinates, and maximum luminance of solution-processed deep-blue OLED devices with CBP host.

Compound	**Emitter conc. (wt%)**	**Turn-on voltage (V)**	**$PE_{max}/CE_{max}/EQE_{max}$ $lmW^{-1}/cdA^{-1}/\%$**	**$PE_{100}/CE_{100}/EQE_{100}$ $lmW^{-1}/cdA^{-1}/\%$**	**CIE coordinates**	**Max. Lum. (cdm^{-2})**
PICFOCz	0.5	3.5	0.2/ 0.2/ 2.2	0.1/ 0.2/ 2.1	(0.16, 0.05)	691
	1	4.5	1.0/ 1.5/ 1.5	0.5/ 0.9/ 1.2	(0.18, 0.14)	763
	3	4.7	0.9/ 1.4/ 1.2	0.5/ 0.9/ 1.1	(0.18, 0.15)	809
	5	5.0	0.5/ 1.0/ 0.7	0.4/ 0.8/ 0.7	(0.21, 0.20)	624
	100	4.4	0.1/ 0.2/ -	-/ 0.1/ -	-	129
BICFOCz	0.5	3.9	0.4/ 0.5/ 3.4	0.2/ 0.3/ 1.7	(0.17, 0.05)	813
	1	5.6	0.2/ 0.3/ 1.4	0.1/ 0.3/ 1.1	(0.17, 0.07)	459
	3	5.6	0.2/ 0.4/ 1.2	0.1/ 0.3/ 1.0	(0.17, 0.08)	418
	5	5.6	0.1/ 0.3/ 1.2	0.1/ 0.3/ 1.0	(0.17, 0.08)	357
	100	5.2	- / - / -	- / - / -	-	29

Turn-on voltage (the voltage at luminance >1 cd/m^2), PE_{max}, CE_{max}, and EQE_{max} represents the maximum power efficiency, current efficiency, and external quantum efficiency of the studied device, respectively. PE_{100}, CE_{100}, and EQE_{100} represent the power efficiency, current efficiency, and external quantum efficiency of the studied device at 100 cd/m^2, respectively. CIE coordinates at 100 cd/m^2.

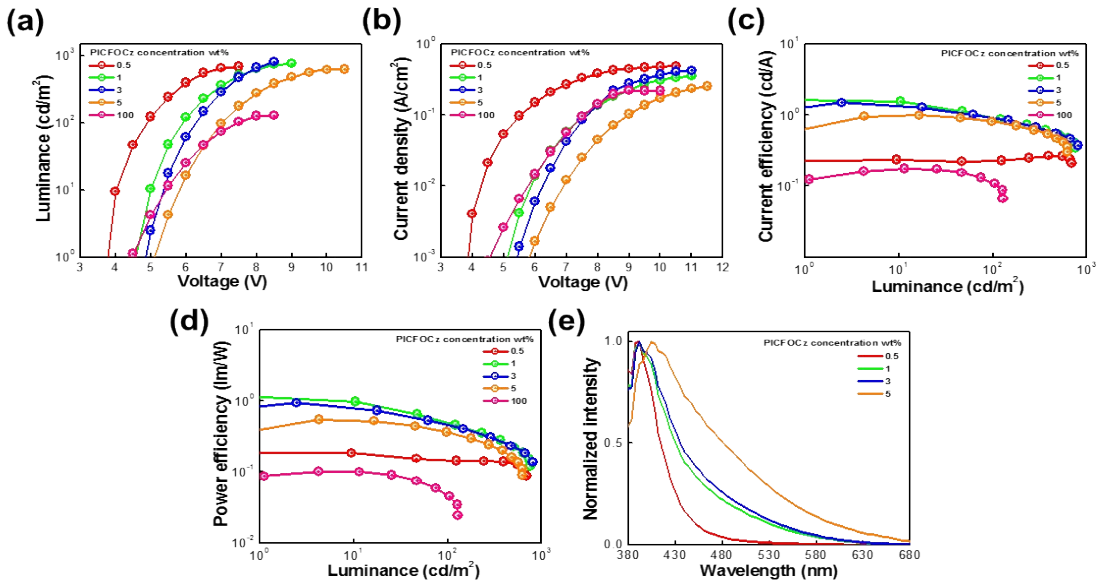

Fig. S21.(a) Luminance-voltage, (b) current density-voltage, (c) current efficiency-luminance, (d) power efficiency-luminance, and (e) normalized EL spectra plots of the solution-processed deep-blue OLED devices based on different doping concentration of PICFOCz within CBP host.

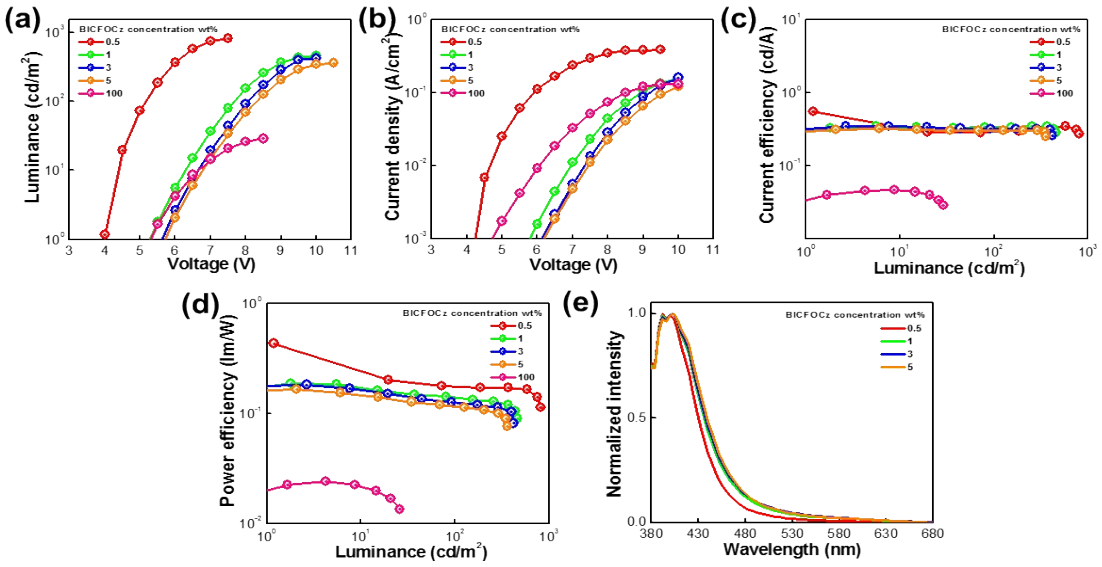

Fig. S22.(a) Luminance-voltage, (b) current density-voltage, (c) current efficiency-luminance, (d) power efficiency-luminance, and (e) normalized EL spectra plots of the solution-processed deep-blue OLED devices based on different doping concentration of BICFOCz within CBP host.

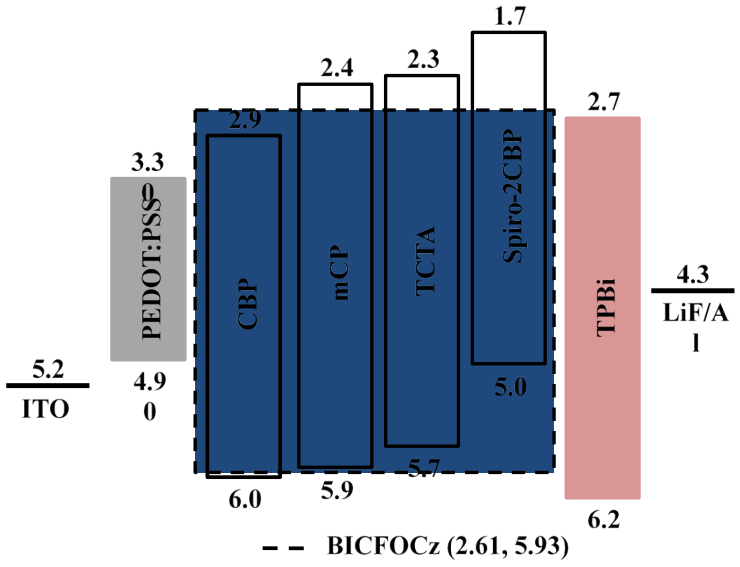

Fig.S23. Schematic illustration of the energy levels of the solution-processed deep-blue OLED devices composing 0.5 wt% BICFOCz emitter in different host molecules, CBP, mCP, TCTA, and Spiro-2CBP.

Table S5. Effect of different hosts on the turn-on voltage, power efficiency (PE), current efficiency (CE), external quantum efficiency (EQE), CIE coordinates, andmaximum luminance of solution-processed 0.5 wt% BICFOCz based deep-blue OLED devices.

Emitter	**Host**	**Turn-on voltage (V)**	**PE_{max}/ CE_{max}/ EQE_{max} (lm W^{-1}/ cd A^{-1}/ %)**	**PE_{100}/ CE_{100}/ EQE_{100} (lm W^{-1}/ cd A^{-1}/ %)**	**CIE coordinates**	**Max. Lum. (cd m^{-2})**
BICFOCz	CBP	3.9	0.4/ 0.5/ 3.4	0.2/ 0.3/ 1.7	(0.17, 0.05)	813
	mCP	6.5	0.2/ 0.3/ 0.9	0.1/ 0.3/ 0.6	(0.18, 0.11)	351
	TCTA	4.1	0.5/ 0.7/ 0.8	0.3/ 0.5/ 0.6	(0.17, 0.11)	1245
	Spiro-2CBP	4.5	0.2/ 0.4/ 2.1	0.1/ 0.2/ 1.6	(0.17, 0.06)	784

Turn-on voltage (the voltage at luminance >1 cd/m^2), PE_{max}, CE_{max}, and EQE_{max} represents the maximum power efficiency, current efficiency, and external quantum efficiency of the studied device, respectively. PE_{100}, CE_{100}, and EQE_{100} represent the power efficiency, current efficiency, and external quantum efficiency of the studied device at 100 cd/m^2, respectively. CIE coordinates at 100 cd/m^2.

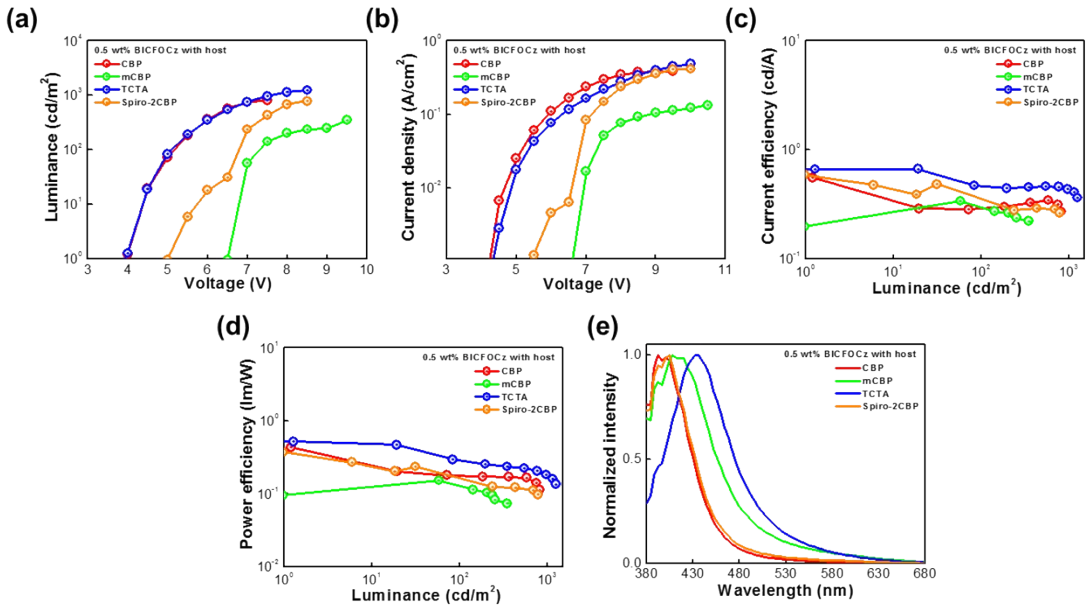

Fig. S24.(a) Luminance-voltage, (b) current density-voltage, (c) current efficiency-luminance, (d) power efficiency-luminance, and (e) normalized EL spectra plots of the 0.5 wt% BICFOCz based solution-processed deep-blue OLED devices in different host matrix.

Table S6. Performance of the solution-processed 0.5 wt% BICFOCz and $Ir(2\text{-phq})_3$ based WOLED devices.

$Ir(2\text{-phq})_3$ (wt%)	**OV (V_{on})**	**$PE_{100}/CE_{100}/EQE_{100}$ (lm W^{-1}/ cd A^{-1}/ %)**	**$PE_{1000}/CE_{1000}/EQE_{1000}$ (lm W^{-1}/ cd A^{-1}/ %)**	**$PE_{max}/CE_{max}/EQE_{max}$ (lm W^{-1}/ cd A^{-1}/ %)**	**CIE_{xy} coordinates**	**Max.Lum. (cd m^{-2})**
0.5	5.0	7.8/13.8/6.3	3.5/7.0/3.5	7.9/13.9/7.0	(0.35, 0.32)	5087
3.0	4.6	11.3/18.7/7.7	4.1/8.6/3.7	13.8/21.9/9.0	(0.44, 0.38)	5589
5.0	4.2	13.6/21.1/8.6	3.9/8.5/3.6	19.7/29.3/11.5	(0.44, 0.38)	6440

Turn-on voltage (the voltage at luminance >1 cd/m^2), PE_{max}, CE_{max}, and EQE_{max} represents the maximum power efficiency, current efficiency, and external quantum efficiency of the studied device, respectively. PE_{100}, CE_{100}, and EQE_{100} represent the power efficiency, current efficiency, and external quantum efficiency of the studied device at 100 cd/m^2, respectively. PE_{1000}, CE_{1000}, and EQE_{1000} represent the power efficiency, current efficiency, and external quantum efficiency of the studied device at 1000 cd/m^2, respectively CIE coordinates at 1000 cd/m^2.

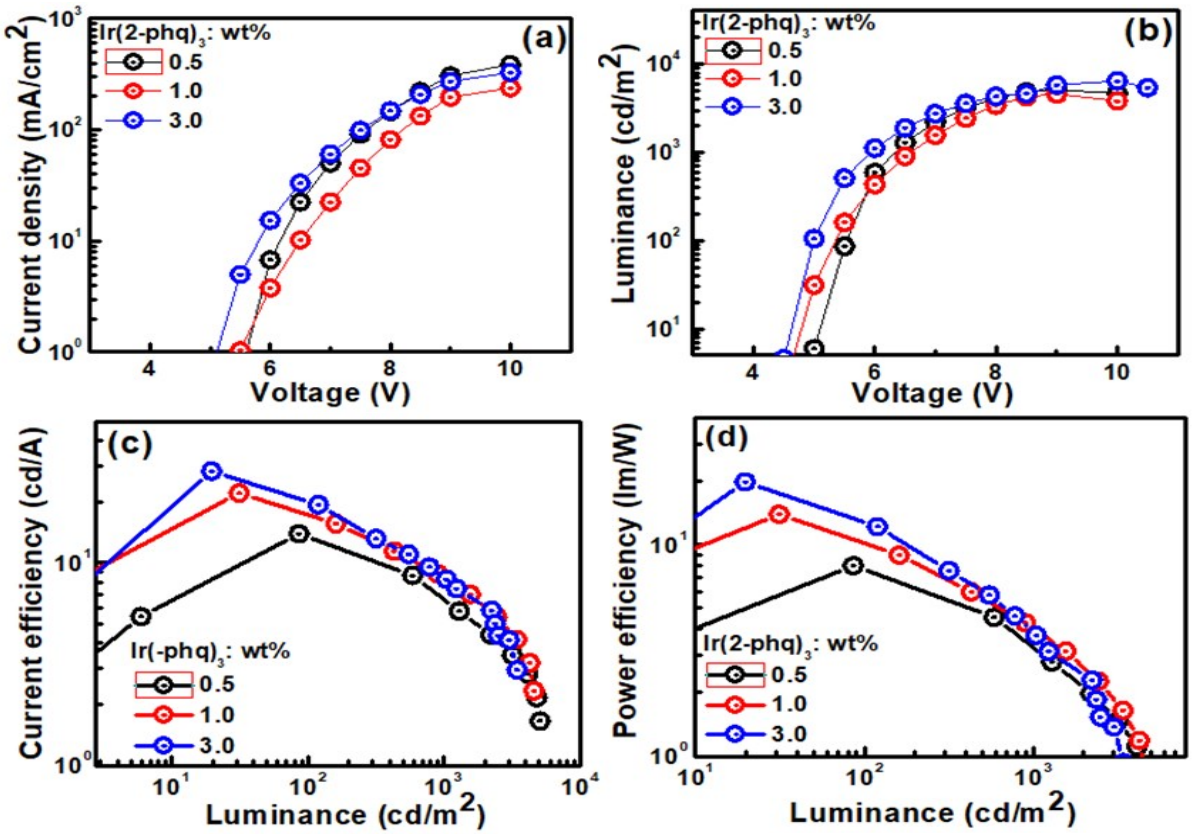

Fig. S25.(a) Current density-voltage, (b) luminance-voltage, (c) current efficiency-luminance, and (d) power efficiency-luminance plots of the solution-processed white-OLED devices using BICFOCz and Ir(2-phq)$_3$ as a near-UV and orange-red, respectively.

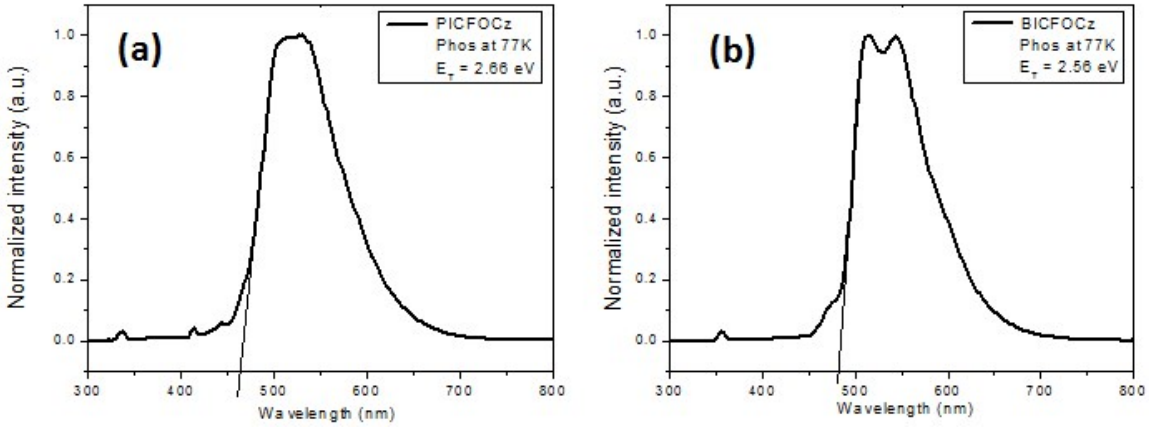

Fig. S26. Phosphorescence spectra of films recorded at 77 K.

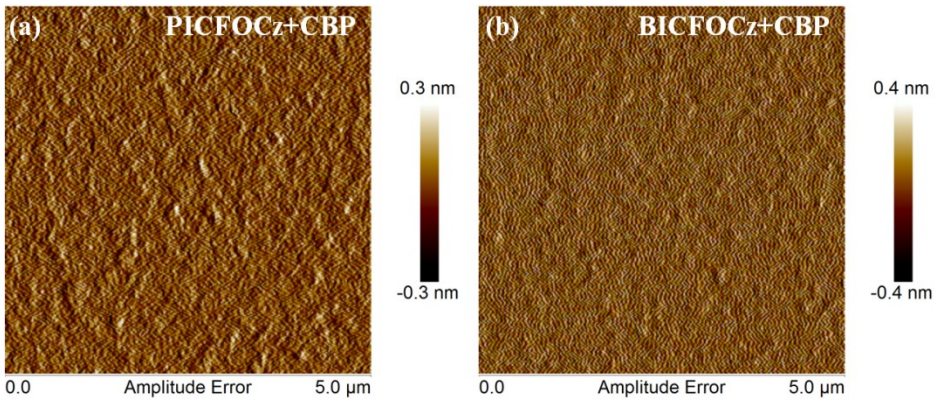

Fig. S27. AFM images of the surface morphology of the films that comprise 0.5 wt% (a) PICFOCz and (b) BICFOCz doped in CBP host matrix.

Table S7. Summary of performance of reported purely organic small molecules based solution-processed blue OLEDs so far.-effect of doping concentration on the operating voltage (OV), power efficiency (PE), current efficiency (CE), external quantum efficiency (EQE), CIE coordinates, and maximum luminance of the solution-processed devices with CBP host. [PE, CE, and EQE at 100 cdm^{-2} and maximum]**.**

Solution-processed EML		Operation voltage (V)	$PE_{max}/CE_{max}/EQE_{max}$ $lmW^{-1}/cdA^{-1}/\%$	$PE_{100}/CE_{100}/EQE_{100}$ $lmW^{-1}/cdA^{-1}/\%$	CIE_{xy} coordinates	Maximum Luminance (cdm^{-2})	Ref
Emitter (Dopant)	**Emitter Concentration (wt%)**						
2,7-CSF	-	3.4	-/0.67/1.71	-/-/-	0.156, 0.054	349	**2**
2,7-CSFX	-	2.8	-/0.89/2.07	-/-/-	0.157, 0.051	886	
3,6-CSFX	-	4.2	-/0.42/0.88	-/-/-	0.251, 0.233	248	
2,7-CSBF	-	3.2	-/1.23/2.49	-/-/-	0.155, 0.050	1332	
5,9-CSBF	-	3.4	-/4.42/4.10	-/-/-	0.150, 0.091	2304	
DPIPOBn	1	9.2	-/-/-	0.2/0.4/0.6	0.16, 0.09	475	**3**
	3	9.3	-/-/-	0.5/0.9/1.6	0.16, 0.10	725	
	5	9.4	-/-/-	0.2/0.6/0.8	0.16, 0.10	508	
	100	9.6	-/-/-	0.1/0.2/0.1	0.29, 0.30	198	
DPITBOBn	1	8.9	-/-/-	0.1/0.3/0.4	0.16, 0.10	549	
	3	9.1	-/-/-	0.5/1.2/1.9	0.16, 0.11	856	
	5	9.4	-/-/-	0.4/0.8/1.2	0.16, 0.11	460	
	100	9.6	-/-/-	0.1/0.2/0.1	0.26, 0.32	178	
PY-II	-	4.5	-/-/-	0.41/0.17/-	(0.16, 0.16)	202	**4**

BIPOCz	0.5	4.1	0.2/ 0.3/ 1.9	0.1/ 0.2/ 1.1	(0.17, 0.07)	434	**5**
	1	4.8	0.3/ 0.5/ 1.5	0.1/ 0.3/ 0.7	(0.18, 0.10)	311	
	3	5.4	0.2/ 0.4/ 1.1	0.1/ 0.2/ 0.5	(0.18, 0.10)	301	
	5	5.4	0.1/ 0.3/ 0.7	0.1/ 0.2/ 0.4	(0.17, 0.09)	349	
	100	4.1	- / - / -	- / - / -	-	67	
BIPTOCz	0.5	4.1	0.1/0.2/ 1.4	0.1/0.2/0.8	(0.17, 0.06)	485	
	1	4.5	0.2/ 0.2/ 1.4	0.1/ 0.2/ 0.9	(0.17, 0.06)	450	
	3	4.7	0.1/ 0.2/ 1.4	0.1/ 0.2/ 0.7	(0.17, 0.08)	381	
	5	4.7	0.1/ 0.2/ 0.8	0.1/ 0.2/ 0.3	(0.13, 0.07)	373	
	100	4.6	- / - / -	- / - / -	-	49	
BITBOCz	0.5	4.1	0.1/ 0.2/ 1.5	0.1/ 0.2/ 0.9	(0.17, 0.06)	474	
	1	4.2	0.2/ 0.3/ 1.3	0.1/ 0.2/ 1.0	(0.17, 0.06)	454	
	3	4.6	0.2/ 0.3/ 1.1	0.1/ 0.2/ 0.7	(0.17, 0.07)	408	
	5	4.7	0.1/ 0.3/ 1.0	0.1/ 0.2/ 0.5	(0.17, 0.08)	374	
	100	4.7	- / - / -	- / - / -	-	21	
BIFOCz	0.5	4.1	0.2/ 0.3/ 1.6	0.1/ 0.2/ 0.9	(0.17, 0.07)	437	
	1	4.6	0.2/ 0.2/ 1.4	0.1/ 0.2/ 0.6	(0.18, 0.08)	518	
	3	5.0	0.1/ 0.2/ 0.8	0.1/ 0.1/ 0.4	(0.18, 0.08)	576	
	5	6.5	0.1/ 0.3/ 1.0	0.1/ 0.2/ 0.4	(0.18, 0.09)	619	
	100	4.2	0.1/ 0.1/ 0.1	0.1/ 0.1/ 0.1	(0.25, 0.30)	125	
C3FLA-2		9.2	0.2/ 0.5/ 0.5	- / - / -	0.158, 0.136	645	**6**
C2FLA-1		7.6	0.1/ 0.2/ 0.1	- / - / -	0.199, 0.197	257	**6**
MDP3FL		6.0	0.1/ 0.07/ 0.1	- / - / -	0.159, 0.099	153	**6**
4a		4.9	0.1/ 0.2/ 0.1	- / - / -	0.23, 0.33	156	**7**
4b		4.8	0.2/ 0.4/ 0.1	- / - / -	0.24, 0.41	256	**7**
4c		4.8	0.1/ 0.2/ 0.1	- / - / -	0.26, 0.49	207	**7**
5a		4.5	0.1/ 0.1/ 0.1	- / - / -	0.24, 0.45	277	**7**
8a		-	- / - / -	- / - / -	-	10	**8**
9a		-	- / - / -	- / - / -	-	19	**8**
JV55		5.1	0.1/ 0.1/ 0.2	- / - / -	0.19, 0.16)	215	**9**
TPI-1		9.2	- / - / -	- / - / -	-	8	**10**
TPI-2		9.0	- / - / -	- / - / -	-	11	**10**

SI11. Atom coordinates of imidazole derivatives.

PICFOCz:

6 1.188549000 0.624694000 -0.952578000

6 0.311081000 -0.191299000 -1.680738000

6 0.664874000 1.556403000 -0.046154000

6	-1.061205000	-0.088953000	-1.500385000
1	0.728589000	-0.895710000	-2.393306000
6	-0.713144000	1.649651000	0.128513000
1	1.315789000	2.206550000	0.526733000
6	-1.604979000	0.828934000	-0.581203000
1	-1.708033000	-0.718490000	-2.099110000
1	-1.120979000	2.374707000	0.824353000
6	-5.247327000	0.691762000	-0.101641000
6	-4.886064000	2.000068000	0.193974000
7	-4.046111000	0.065515000	-0.459877000
7	-3.537762000	2.192861000	0.045304000
6	-3.042996000	1.033475000	-0.343766000
6	-5.851973000	2.984753000	0.587953000
6	-5.474528000	4.314918000	0.860832000
6	-7.211861000	2.577917000	0.688556000
6	-6.423301000	5.250219000	1.228727000
1	-4.425742000	4.578919000	0.769987000

6	-8.154126000	3.563786000	1.064743000
6	-7.772518000	4.868281000	1.328965000
1	-6.129378000	6.275445000	1.437181000
1	-9.204662000	3.309805000	1.151141000
1	-8.524325000	5.598976000	1.615085000
6	-6.598686000	0.213112000	0.023249000
6	-7.583419000	1.183282000	0.416900000
6	-7.000130000	-1.126471000	-0.190682000
6	-8.918741000	0.742022000	0.547599000
6	-8.319701000	-1.514931000	-0.047590000
1	-6.263651000	-1.870398000	-0.462366000
6	-9.289517000	-0.571635000	0.319821000
1	-9.687012000	1.446852000	0.843721000
1	-8.598057000	-2.551712000	-0.216073000
1	-10.328428000	-0.868340000	0.434000000
6	-3.862142000	-1.305044000	-0.824060000
6	-4.222568000	-1.740543000	-2.103739000

6	-3.317057000	-2.199910000	0.097938000
6	-4.041580000	-3.077472000	-2.457005000
1	-4.646528000	-1.029598000	-2.806223000
1	-3.047358000	-1.854003000	1.089185000
6	-3.496558000	-3.977431000	-1.541391000
1	-4.327061000	-3.418301000	-3.447631000
6	-3.133694000	-3.534934000	-0.266442000
6	3.468099000	1.242194000	-0.496171000
1	3.295492000	2.304450000	-0.717828000
1	3.348669000	1.095712000	0.587272000
6	4.860219000	0.820425000	-0.945851000
1	4.938271000	0.974440000	-2.030240000
1	5.584324000	1.496940000	-0.475799000
6	5.194436000	-0.634283000	-0.595084000
1	5.084537000	-0.783493000	0.487306000
1	4.472062000	-1.301760000	-1.079779000
6	6.606692000	-1.069611000	-1.018991000

8	2.515844000	0.441748000	-1.199865000
6	10.213453000	2.757671000	-1.420962000
6	9.271677000	2.340016000	-2.376847000
6	8.375445000	1.306630000	-2.111230000
6	8.441872000	0.687753000	-0.858355000
6	9.389674000	1.098445000	0.117946000
6	10.275867000	2.141367000	-0.174377000
1	10.896574000	3.567997000	-1.658869000
1	9.237148000	2.833256000	-3.344580000
1	7.650504000	1.001529000	-2.859639000
1	11.005243000	2.464457000	0.564055000
6	8.124398000	-0.631914000	0.949127000
6	7.676408000	-1.599912000	1.854267000
6	8.305802000	-1.669677000	3.095723000
6	9.354773000	-0.798053000	3.435049000
6	9.798452000	0.162872000	2.530376000
6	9.185711000	0.253656000	1.275540000

1	6.865955000	-2.278977000	1.606937000
1	7.975137000	-2.413859000	3.815300000
1	9.822720000	-0.877235000	4.412146000
1	10.612226000	0.833538000	2.794322000
1	6.734178000	-2.141661000	-0.825413000
1	6.740283000	-0.930027000	-2.096600000
7	7.682095000	-0.360081000	-0.342311000
1	-3.360211000	-5.019741000	-1.809827000
6	-2.497606000	-4.500473000	0.700386000
9	-2.662472000	-4.114139000	1.982518000
9	-1.166943000	-4.611921000	0.485830000
9	-3.019803000	-5.740928000	0.575651000

BICFOCZ:

6	1.429440000	0.249617000	-0.612336000
6	0.477843000	-0.714353000	-0.975646000
6	0.999902000	1.469072000	-0.072359000
6	-0.876377000	-0.469690000	-0.795286000
1	0.823424000	-1.645473000	-1.413803000
6	-0.361741000	1.702128000	0.108828000

1	1.710634000	2.237425000	0.209336000
6	-1.324932000	0.742126000	-0.236677000
1	-1.587855000	-1.222321000	-1.115793000
1	-0.698028000	2.649262000	0.517319000
6	-4.961014000	0.979721000	0.257191000
6	-4.552063000	2.289059000	0.048529000
7	-3.785014000	0.216081000	0.200606000
7	-3.190953000	2.331137000	-0.151608000
6	-2.742682000	1.095256000	-0.060341000
6	-3.696885000	-1.188642000	0.443915000
6	-4.350555000	-2.086443000	-0.403509000
6	-2.959326000	-1.660630000	1.534232000
6	-4.260662000	-3.456560000	-0.154988000
1	-4.919452000	-1.716739000	-1.248397000
1	-2.459709000	-0.951306000	2.185952000
6	-3.515222000	-3.934915000	0.926009000
1	-3.442149000	-5.002905000	1.102036000
6	-2.864783000	-3.032483000	1.766104000
6	3.753660000	0.864811000	-0.532930000
1	3.592817000	1.775632000	-1.126118000
1	3.711002000	1.139526000	0.531355000
6	5.097511000	0.233497000	-0.871095000
1	5.095635000	-0.040647000	-1.934278000

1	5.871928000	0.999163000	-0.741378000
6	5.421104000	-0.993456000	-0.010827000
1	5.403028000	-0.709806000	1.049987000
1	4.640164000	-1.750896000	-0.147959000
6	6.777398000	-1.642507000	-0.332535000
8	2.732280000	-0.089381000	-0.829168000
6	10.408844000	1.517274000	-2.487492000
6	9.374028000	0.812120000	-3.125448000
6	8.486372000	0.014730000	-2.405841000
6	8.657112000	-0.069375000	-1.019881000
6	9.699926000	0.636825000	-0.361048000
6	10.575383000	1.433099000	-1.108103000
1	11.082442000	2.132190000	-3.077435000
1	9.259103000	0.890039000	-4.203262000
1	7.689364000	-0.517918000	-2.915392000
1	11.376551000	1.978411000	-0.615737000
6	8.483220000	-0.559403000	1.179890000
6	8.102151000	-1.070773000	2.424974000
6	8.843529000	-0.685700000	3.540512000
6	9.936934000	0.189846000	3.426458000
6	10.313468000	0.695379000	2.184962000
6	9.588039000	0.323264000	1.047623000
1	7.258509000	-1.746528000	2.528354000

1	8.566728000	-1.070757000	4.518312000
1	10.492593000	0.472362000	4.316066000
1	11.161905000	1.369547000	2.099533000
1	-2.283715000	-3.397494000	2.607639000
1	6.895839000	-2.558561000	0.258918000
1	6.813597000	-1.944668000	-1.384153000
7	7.928094000	-0.789351000	-0.075477000
6	-5.332998000	3.539928000	0.032721000
6	-4.829507000	4.646328000	-0.673599000
6	-6.546784000	3.685165000	0.725752000
6	-5.527552000	5.851503000	-0.701763000
1	-3.882530000	4.543431000	-1.192984000
6	-7.243723000	4.892277000	0.693914000
1	-6.940236000	2.856872000	1.305165000
6	-6.740844000	5.980187000	-0.022051000
1	-5.122578000	6.693640000	-1.257422000
1	-8.179100000	4.984462000	1.240157000
1	-7.285463000	6.920508000	-0.044527000
6	-6.297364000	0.385242000	0.457159000
6	-7.299766000	0.585573000	-0.508034000
6	-6.606995000	-0.374891000	1.598096000
6	-8.572412000	0.043438000	-0.336136000
1	-7.071497000	1.173223000	-1.392223000

6	-7.878496000	-0.923106000	1.764172000
1	-5.849657000	-0.529194000	2.361122000
6	-8.865245000	-0.715889000	0.798639000
1	-9.334058000	0.209156000	-1.093316000
1	-8.099548000	-1.508255000	2.652834000
1	-9.855810000	-1.142733000	0.930008000
6	-5.013584000	-4.426491000	-1.027891000
9	-6.224804000	-4.726152000	-0.506424000
9	-5.226977000	-3.931717000	-2.265984000
9	-4.346345000	-5.594532000	-1.164747000

References:

1. J. Jayabharathi, P. Ramanathan, V. Thanikachalam and C. Karunakaran, *New J. Chem.* 2015, **39**, 3801-3812.
2. P. Therdkatanyuphong, C. Kaiyasuan, P. Chasing, T. Kaewpuang, T. Chawanpunyawat, P. Wongkaew, T. Sudyoadsuka and V. Promaraka, Mater. Chem. Front., 2020, 4, 2943-2953.
3. J. Tagare, D. K. Dubey, J. H. Jou and S. Vaidyanathan, *ChemistrySelect,* 2019, **4**, 6458 – 6468
4. N. G. Valsange, F. L. Wong, D. Shinde, C. S. Lee, V. A. L. Roy, S. Manzhos, K. Feron, S. Chang, R. Katoh, P. Sonar and P. P. Wadgaonkar, *New J. Chem*., 2017, **41**, 11383.
5. J. Tagare, R. Boddula, R. A. K. Yadav, D. K. Dubey, J. H. Jou, S. Patel and S. Vaidyanathan, Dyes and Pigments, 2021, 185, 108853.
6. Y.-C. Wang, T.-H. Li and H.-H. Yu, *Journal of Materials Chemistry C*, 2015, **3**, 2182-2194.

7. V. Joseph, K. R. Justin Thomas, W. Y. Yang, R. A. Kumar Yadav, D. Kumar Dubey and J.-H. Jou, *Asian Journal of Organic Chemistry*, 2018, **7**, 1654-1666.
8. I. Bala, W.-Y. Yang, S. P. Gupta, J. De, R. A. K. Yadav, D. P. Singh, D. K. Dubey, J.-H. Jou, R. Douali and S. K. Pal, *Journal of Materials Chemistry C*, 2019, **7**, 5724-5738.
9. J.-H. Jou, J.-L. Li, S. Sahoo, D. K. Dubey, R. A. Kumar Yadav, V. Joseph, K. R. J. Thomas, C.-W. Wang, J. Jayakumar and C.-H. Cheng, *The Journal of Physical Chemistry C,* 2018. **122**, 24295-24303.
10. A. B. Kajjam, D. K. Dubey, R. A. Kumar Yadav, J.-H. Jou and V. Sivakumar, *Materials Today Chemistry,* 2019, **14**, 100201.